Renewable and Sustainable Energy Reviews 109 (2019) 349–366

Contents lists available at ScienceDirect

Renewable and Sustainable Energy Reviews

journal homepage: www.elsevier.com/locate/rser

Recent advances in direct expansion solar assisted heat pump systems: A review

Guo-Hua Shi[a,b,*], Lu Aye[b], Dan Li[a], Xian-Jun Du[c]

[a] Department of Energy and Power Engineering, North China Electric Power University, Baoding, 071003, China
[b] Renewable Energy and Energy Efficiency Group, Department of Infrastructure Engineering Melbourne School of Engineering, The University of Melbourne, Victoria, 3010, Australia
[c] College of Electrical and Information Engineering, Lanzhou University of Technology, Lanzhou 730050, China

ARTICLE INFO

Keywords:
Solar assisted heat pump
Ambient energy
Configurations
Thermal performance
Applications

ABSTRACT

Direct-expansion solar assisted heat pumps (DX-SAHPs) have a great potential for various applications and are conductive to the environment by using low-temperature ambient energy and solar radiation. This review paper aims at presenting the advancements and the current status of DX-SAHPs. A systematic literature review highlights and discusses various aspects of this technology, including system configurations, performance optimisation, simulation models, and various applications in practice. This review indicates that integrating solar collector-evaporators with some advanced technologies, such as photovoltaic, PCM thermal storage and heat pipe, makes DX-SAHPs perform better under different climates and applications. This study concludes that there are clear trends for promoting commercialisation prospects of the technology with introducing DX-SAHPs into various industries and exploring multi-functional applications of DX-SAHPs. To realise greater commercial success, some suggestions for further research are also made. This review work is expected to serve as a good guide for researchers working or interested in the DX-SAHP field.

1. Introduction

With the increasing concerns on environmental problems and fossil energy depletion, improving energy efficiency and accelerating deployments of renewable energy have received great attention around the world. Solar energy is generally acknowledged as the most abundant and effective form of renewable energy and it is being applied directly or indirectly in various places in the world.

Direct-expansion solar assisted heat pump (DX-SAHP), as a technology of low-temperature solar thermal conversion proposed first by Sporn and Ambrose in 1955 [1], can be regarded as an important expansion of solar thermal utilisation technologies as well as heat pump applications. In DX-SAHP systems, a critical component known as a collector-evaporator integrates the functions of collecting solar energy and vaporising liquid refrigerant (working fluid). In comparison to the equivalent traditional flat plate solar collector, the collector-evaporator is simpler and cheaper because it does not require glazing or cover to reduce heat losses. Refrigerant as the working fluid in the solar collector eliminates the corrosion and freeze problems that often occur in conventional solar collectors with water as the heat transfer fluid. Additionally, inside the collector-evaporator, the circulation and direct expansion of refrigerant reduces its surface temperature significantly. This reduces heat losses of the collector to the surroundings and possibly even helps the collector obtain thermal energy from ambient air in some cases.

Because of these distinctive advantages, the interest in the DX-SAHP technology began to be renewed in the 1970s after the oil crisis. Charters and Taylor [2] at the University of Melbourne proposed to use an unglazed flat-plate solar collector as the evaporator of a DX-SAHP system in 1976. In the next year, Franklin et al. [3] developed an unglazed solar collector-evaporator with a reflector on the back that absorbed solar energy by its two sides and contributed to a high thermal performance of the DX-SAHP system. Since then, many researchers have carried out studies on DX-SAHP systems for half a century. It was found that the concentration of research is in the Pacific Rim and the Southern Europe (Fig. 1) based on the current literature review. The reasons may be related to abundant solar resource, impressive GDP growth, and increasing energy demand, as well as more proactive policies on renewable energy in these regions.

This investigation presents a detailed literature review and the major developments of DX-SAHP systems. The review presents various aspects on configurations, optimal design, dynamic simulation models

* Corresponding author. Department of Energy and Power Engineering, North China Electric Power University, Baoding, 071003, China.
E-mail addresses: g.h.shi@ncepu.edu.cn, ghuashi@outlook.com (G.-H. Shi).

https://doi.org/10.1016/j.rser.2019.04.044
Received 2 January 2018; Received in revised form 23 March 2019; Accepted 13 April 2019
Available online 20 April 2019
1364-0321/

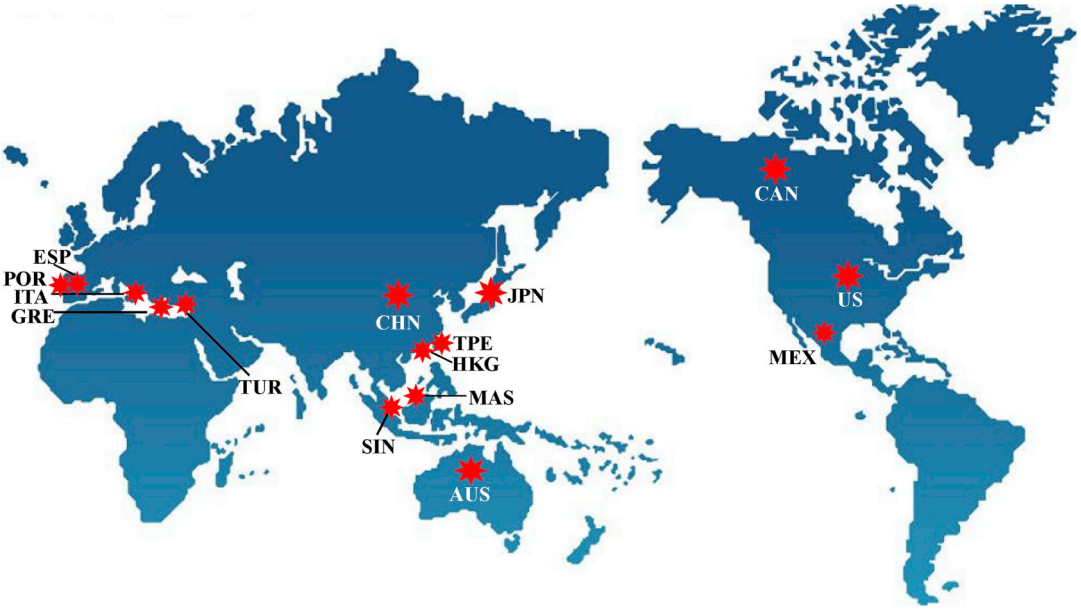

Fig. 1. Countries conducting researches on DX-SAHP.

and practical applications. It is expected that the review assists to increase awareness of this solar thermal conversion technology and to enhance efforts to expand its commercial applications.

2. System description and thermal performance criteria

As illustrated in Fig. 2, a DX-SAHP consists of a collector-evaporator, a compressor, a condenser and an expansion valve, which are linked to form a closed circuit by copper tubes filled with refrigerant. Liquid refrigerant with low temperature and pressure is delivered into a solar collector-evaporator from an expansion device and directly vaporizes by receiving heat from incident solar radiation and/or ambient air. Then a compressor provides mechanical work to the superheated refrigerant vapour arriving from the solar collector and then increases its pressure and temperature. After compression, the refrigerant vapour flows into a condenser and releases heat to become the saturated/subcooled liquid refrigerant. Subsequently, the expansion device reduces the pressure of liquid refrigerant from the condenser outlet. Then the low-pressure liquid refrigerant enters the collector-evaporator, and the cycle repeats.

Coefficient of performance (COP) is an efficiency indicator to evaluate the performance of DX-SAHP and is defined as the ratio of the thermal energy rejected by the condenser over a specified time period to the electrical energy input to the compressor over the same time period [4]. Based on the first law of thermodynamics as well as the assumption that heat losses of the condenser are negligible, it is usually expressed as follows:

$$\mathrm{COP} = \frac{F_{\mathrm{R}} A_{\mathrm{CE}} [I_{\mathrm{s}}(\tau\alpha) - U_{\mathrm{L}}(T_{\mathrm{CE}} - T_{\mathrm{A}})] + W_{\mathrm{Comp}}}{W_{\mathrm{Comp}}} \quad (1)$$

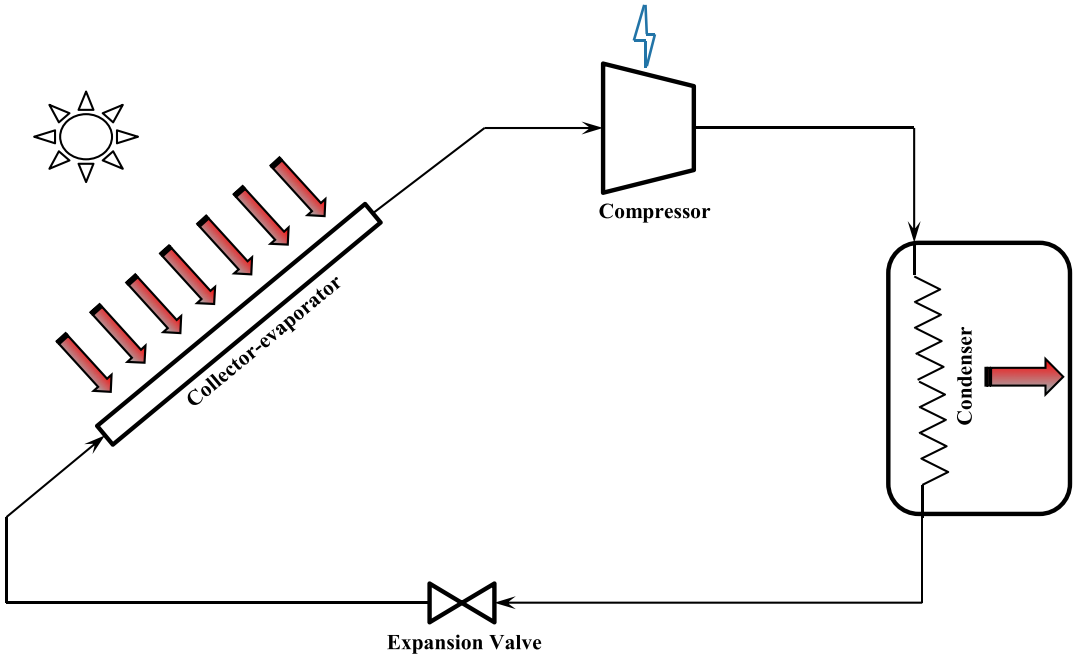

Fig. 2. Schematic of DX-SAHP.

where, F_R is the collector efficiency factor, A_{CE} is the collector-evaporator area, I_s is the solar radiation intensity on the collector surface, $\tau\alpha$ is the effective absorptivity, U_L is the heat loss coefficient of collector, T_{CE} is the evaporation temperature, T_A is the ambient temperature, and W_{Comp} is the electrical work input to the compressor. It is obvious that if there is no solar radiation, a DX-SAHP will work as an air-source heat pump which evaporation temperature is lower than the ambient temperature.

Another performance criterion is solar collector efficiency that is defined as the ratio of the useful energy collected by the collector over a specified time period to the incident solar energy in the collector plane over the same time period and is written as [4]:

$$\eta = \frac{F_R A_{CE}[I_s(\tau\alpha) - U_L(T_{CE} - T_A)]}{I_s A_{CE}} \quad (2)$$

As seen from Eqs. (1) and (2), for a specified solar radiation intensity, DX-SAHP systems will gain better performance under the conditions of negative temperature differences between refrigerant in the collector and ambient air.

3. Various configurations of DX-SAHPs

3.1. Split type and integral type DX-SAHP

The split type solar-assisted heat pump is the main form existing in a large number of studies. It includes a collector-evaporator installed outside to obtain heat from the sun or ambient air, and the other three components inside building. Its major advantages are the high layout flexibility and the integration of the collector-evaporator with buildings. However, it is apparent that the connection among the collector-evaporator and other parts together requires longer copper tubes. Additionally, the inside components take up too much indoor space.

In order to install a DX-SAHP easily without space restriction and reduce its overall cost, Huang and Chyng (1999) proposed the design of an integral-type solar-assisted heat pump (ISAHP) water heater that combines a solar collector, a heat pump and a water storage tank together as a single package [5]. Fig. 3(a) shows that the unglazed solar collector with a selective black surface is laid on the top, the front and the two sides of ISAHP and acts as a part of shell wall [6]. For Scarpa et al.'s ISAHP [7] (as shown in Fig. 3(b)), the unglazed solar collector with an adjustable slope can absorb more solar thermal energy in different latitude areas. It is clear that an ISAHP is more compact in size and has a larger market potential as compared to a split-type DX-SAHP. Moreover, both experimental and theoretical research results proved it has a good thermal performance on generating hot water at temperatures between 30 and 61 °C [5–9]. The ISAHP obtained high COP values about 7.0 under the weather conditions of Italy by use of the optimised control policy [7] and worked with a system COP value greater than 2.0 for most of the year in Taipei [8].

3.2. Collector-evaporator

3.2.1. Glazed and unglazed collector-evaporators

The collector-evaporator is an essential component of DX-SAHP. Due to the circulation of refrigerant in the collector, the collector operating temperature is slightly above and sometimes even lower than the ambient temperature. Therefore, the unglazed flat plate collector without insulation on the back is the most common type applied. This type can also obtain sensible heat from ambient air and even the latent heat of water vapour in the case of condensation of moisture within the air. Tagliafico et al. [10] compared thermodynamic performance of three solar collector configurations (unglazed, single or double glazed panels) and found that the annual primary energy savings of DX-SAHP were 49.5%, 48.5% and 48%, respectively. It may be concluded that the savings on primary energy consumption is not strongly dependent on the type of collector-evaporator and the unglazed one (the cheapest one among these configurations) is a good choice for DX-SAHP.

3.2.2. Various designs in material, size and flow channel pattern of collector-evaporators

Some exergy studies on DX-SAHP showed that the collector-evaporator has the highest exergy destruction [11–13]. Consequently, many research works have focused on the design of collector-evaporators and some influencing factors to increase the overall performance.

Copper and aluminium are regarded as ideal materials for manufacturing solar collectors because of their good thermal conductivity and high ductility properties. The work of Zhang et al. [14] showed that copper, with higher thermal conductivity, can increase the thermodynamic performance of DX-SAHP in comparison with aluminium, however, the increment in COP is very small (only 0.5% increase for a solar collector plate thickness of 1 mm) and is negligible for plate

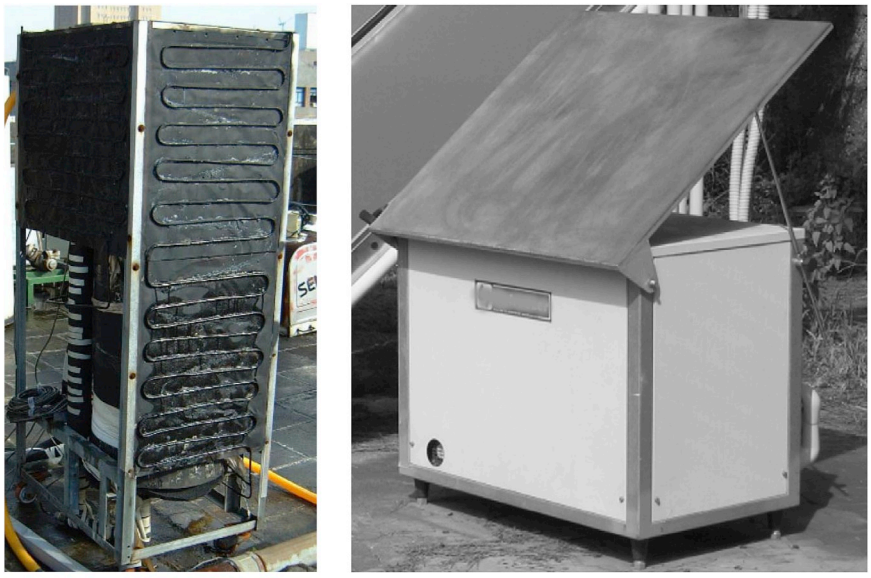

(a) (b)

Fig. 3. Prototypes of different ISAHPs. (a) ISAPH by Huang et al. [6]; (b) ISAHP with an instantaneous gas burner by Scarpa et al. [7].

thicknesses higher than 5 mm. So aluminium was widely used for making collector plates in many previous studies because of its lower price. Increasing collector plate thickness offers a high system thermal performance as well as a good stability. But Zhang et al. [14] suggested that the maximum thickness is 4 mm above which the values of COP and collector efficiency have no significant increase for the collector.

The flow channel pattern can affect the performance of a roll-bond evaporator. Sun et al. [15] investigated and compared the thermal performance of both the evaporator and the DX-SAHP with three different channel patterns (i.e. parallel shape, fractal T-shape and honeycomb shape) under the same cross section area. The hexagon shaped channel is the optimal geometric structure for a roll-bond panel to maximise the evaporating temperature. Compared to the other two channel patterns, the honeycomb-type channel increases COP of the DX-SAHP water heating system by 21.4% and 5.9%, respectively, because it has the lowest thermal resistance between the collector plate and the refrigerant [15].

3.2.3. Heat-pipe collector-evaporators

With the purpose of reducing electricity consumption and achieving higher energy efficiency, Huang et al. [16] combined a solar heat pipe collector and a DX-SAHP water heater (DX-SAHPWH), and presented a heat-pipe enhanced solar-assisted heat pump water heater (abbreviated to HPSAHP). The novel system works as a conventional heat pump in the case of low solar radiation, while it operates in the heat-pipe mode during high solar radiation. In the heat-pipe mode operation, refrigerant after absorbing thermal energy in the collector enters the condenser directly without running compressor and heats water. The research results concluded that the operation of HPSAHP should switch from the conventional heat-pump mode to the heat-pipe mode when the water temperature is less than 30 °C and the solar radiation intensity is greater than 400 W m^{-2}. As a result of the combination of the two modes, the COP of HPSAHP is 3.32 and increases by 28.7% as compared to the small ISAHP designed by Huang and Chyng in Ref. [8].

3.2.4. Collector-evaporators with spiral-finned tubes

On cloudy or rainy days when low solar radiation cannot yield enough heat for water-heating, integrating a DX-SAHP and an air-source heat pump is a good and practical idea for solving such a problem [17]. An integrated solar-air source heat pump water heater (SAS-HPWH) designed by Xu et al. [18] significantly differs from a traditional DX-SAHPWH because it has a special flat plate collector-evaporator with spiral-finned tubes. The collector plate surface is used to collect solar thermal energy, while the copper-aluminium spiral-finned tubes absorb adequate thermal energy from ambient air by convection heat transfer when the ambient temperature is higher than the evaporating temperature. Therefore, the SAS-HPWH can also operate even on rainy days or in the evenings by using air-source energy only. The simulated results showed that the SAS-HPWH took about 8.8 h to heat water from 15 to 55 °C with an average COP value of 3.3 on overcast and rainy days in winter when the values of ambient temperature and solar radiation were 5 °C and 50 W m^{-2}, respectively.

3.2.5. PV collector-evaporators

A novel combined photovoltaic solar assisted heat pump (PV-SAHP) system was presented in which a specially designed direct expansion solar collector with PV cells laminated on the front surface was adopted to act as a PV evaporator for the production of both electricity and thermal energy [19]. As illustrated in Fig. 4, the mucilage glued aluminium plate has an array of grooves shaped like Ω and is adhered to the aluminium-alloy base plate. The refrigerant tube in copper is firmly fixed between the two plates. PV cells are packed between two transparent tedlar polyester-tedlar (TPT) layers over which internal surface ethylene-vinyl acetate (EVA) spreads evenly and then are placed on the top surface of the base plate. In order to obtain better electrical isolation and good thermal conduction, PV cells, TPT, EVA and the base plate are laminated by a vacuum-laminating machine. The PV evaporator is insulated on its back. The evaporator is installed in an aluminium frame with a removable glass cover. Apart from acting as a concentrating lens, the glass cover can reduce the heat losses of the evaporator upper surface and offer better mechanical protection. The photovoltaic module efficiency can be improved due to the lower working temperature of PV cells caused by a greater cooling effect on the evaporator. At the same time, the evaporating temperature and pressure will rise because of the more solar energy absorption, which is beneficial for improving the system COP.

Subsequently, extensive research works were conducted in Hefei city, China [20–22]. All these works reported that the PV-SAHP system has the considerably higher thermal or photovoltaic performance as compared to a conventional heat pump water heater or a conventional photovoltaic system. The simulation results conducted by Pei et al. [19] indicated that area, tilt angle and refrigerant tube pitch of PV evaporator are important design parameters which greatly affect both the electrical efficiency and the thermal performance of PV-SAHP. Mastrullo and Renno [23] developed a theoretical model of PV-SAHP systems in Southern Italy from the thermoeconomic point of view. Results from the model further demonstrated that the PV heat pump has a higher COP value (varying from 4.5 to 8.4) than a traditional heat pump under the same working conditions. Additionally, the PV-SAHP systems with a simple pay-back period of about four years, both for domestic water heating and for space cooling in summer, is deemed to be economically better than conventional heat pump systems in the long term.

3.2.6. Heat-pipe PV/T collector-evaporators

A hybrid system combining a PV-SAHP system with a heat-pipe system was further presented and was known as a PV-SAHP/HP system for full use of advantages of these two systems [24]. The novel heat-pipe PV/T collector-evaporator has heat pipes in which water flows and a refrigerant tube bonded with the back of the aluminium base plate. Hence, this collector-evaporator makes the PV-SAHP/HP system choose a water-circulation loop or a refrigerant-circulation loop to operate optimally according to different solar radiation levels. The experimental results indicated that the PV-SAPH/HP system can meet domestic hot water requirements with significantly lower power consumption and the daily average values of COP are 3.32–4.01 under different daily total solar radiation ranging from 48.4 to 102.8 MJ [24].

3.2.7. Collector-evaporators with PCM energy storage

Thermal energy storage using phase change materials (PCMs) is an attractive way to solve main issues of solar thermal systems, such as the time difference between solar availability and thermal consumption of users, low efficiency and unstable operation on rainy days. Wu et al. [25] proposed an energy collection/energy storage/evaporation integrated solar heat pump water heater (SHPWHICSE) in 2009. The innovation of the system is a special solar collector that combines solar energy collection, thermal storage and evaporation of refrigerant in one as shown in Fig. 5. PCMs fill the space between the inner wall of the evacuated collector tube and the outer wall of the copper refrigerant tube. There are brushes on the U-shape evaporator tube to eliminate the uneven distribution of PCMs that may result from the density change. Due to the introduction of PCMs, excess thermal energy can be stored by means of the solid-liquid phase change in the case of high solar radiation or low heat demand. The stored energy will be as a heat source to vaporise the refrigerant flowing through the copper tube and then to drive the operation of the heat pump when there is little or no solar radiation. A series of theoretical and experimental works demonstrated that the SHPWHICSE using paraffin or decanoate as PCMs is more stable and efficient in comparison with a conventional DX-SAHPWH [25–30]. For instance, the average COP values of SHPWHICSE were 4.13 and 4.24 on a rainy day with an average solar radiation intensity of 230 W m^{-2} and an average ambient temperature of 12.6 °C

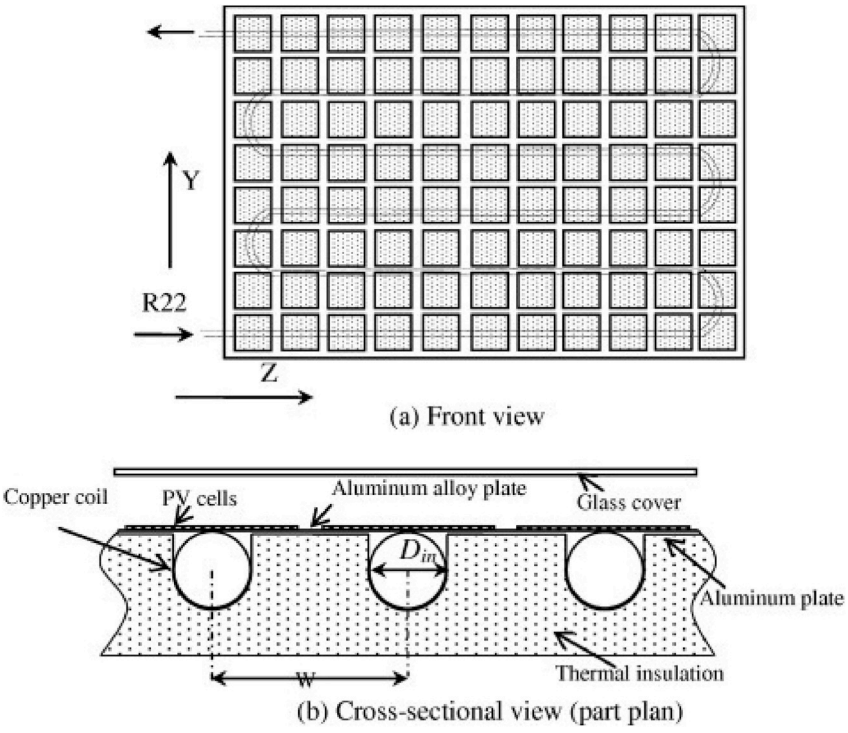

Fig. 4. (a) Front view of PV evaporator [22]; (b) Cross-section of PV evaporator [22].

and at night with an average ambient temperature of 18.0 °C, respectively [26].

3.2.8. Collector-evaporators integrated with LNG tubes

As mentioned before, when the plate temperature is lower than that of ambient air, the refrigerant inside the collector will capture the heat from ambient air. In a hybrid system which combines a DX-SAHP and ambient air vaporisers of LNG (liquefied natural gas) proposed by Shi [31] (see the description of the system in Section 6.4), an evaporator refrigerant tube is tightly fastened between a mucilage glued aluminium plate and an aluminium base plate with selective absorbing coating. What makes the collector-evaporator unique is that an LNG tube in Ni alloy steel is set inside the refrigerant tube, i.e. the two tubes are in the form of a concentric sleeve. A certain amount of cryogenic LNG will flow through the LNG tube and absorb heat from the refrigerant in order to keep the collector temperature always lower than the ambient temperature as well as to increase the temperature of the cryogenic liquid before entering LNG ambient air vaporisers. It is apparent that this design helps the whole system work more effectively even under bad weather conditions.

3.3. Compressor

According to the current review, it is found that both reciprocating-type compressors and scroll compressors had a similar frequency of use in the reported DX-SAHP research works. However, the former was mainly applied in the literature before the year 2007. Huang and Chyng [8] reported that the use of the scroll compressor with a higher volumetric efficiency can increase the system performance. Furthermore, Ozer Kara et al. [32] presented an exergy assessment of a DX-SAHP floor heating system and found that the exergy destruction rate of compressor was 1.18 kW which was four to seven times that of other individual components, while the overall destruction rate was 2.07 kW. The work further indicated that replacing the reciprocating compressor by a scroll compressor contributes to increase the COP of the DX-SAHP floor heating system. Therefore, choosing a scroll compressor may be more appropriate to enhance the thermal performance for DX-SAHP systems.

3.4. Condenser

The condenser transfers heat from high-pressure/temperature refrigerant vapour to a medium (such as water or air) to fulfil the intended applications of DX-SAHP systems. There are not many configurations of condensers as compared to solar collector-evaporators. The reason may be that the condenser is a more conventional heat exchanger.

When a DX-SAHP is applied to produce hot water, a condenser being installed directly inside a water tank (i.e. immersion condenser) is the most common type due to its simple structure [7,12,14–16,24,33–46]. Some designers wrap and solder condenser copper coils on the storage tank surface [47,48]. When the wrap-around coil worked as a condenser, Anderson and Morrison [48] suggested that it should be located in the lower part of the tank in order to improve the system

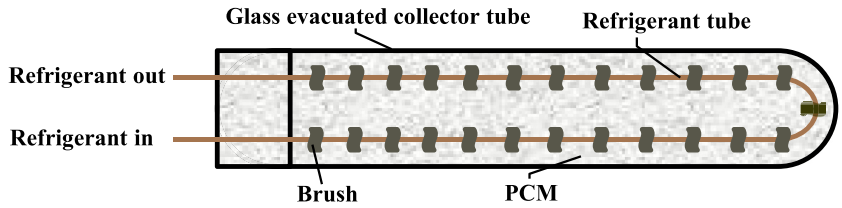

Fig. 5. Structure of the solar collector (part plan).

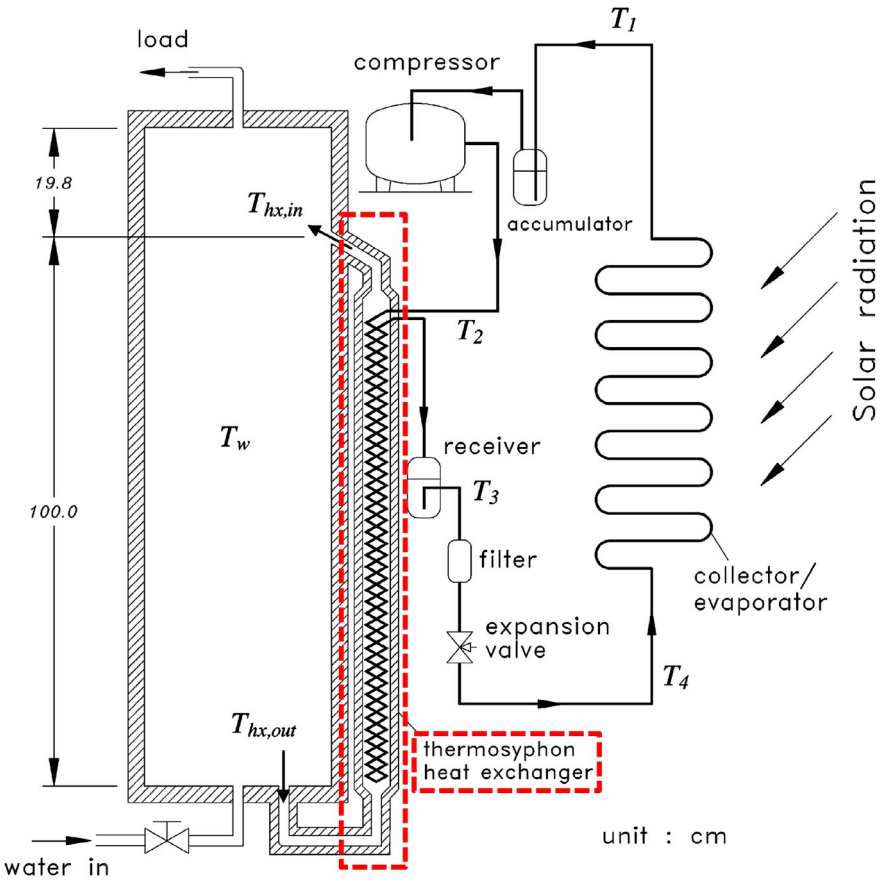

Fig. 6. Thermosyphon heat exchanger in the ISAHP [9].

performance.

A counter-flow tube-in-tube heat exchanger is another popular type of condensers used in DX-SAHP systems for ensuring good heat transfer performance between refrigerant and water [18,25–30,49,50]. The water and the refrigerant circulate in the outer section loop and the inner section loop, respectively. This enhances the total heat transfer coefficient in comparison with an immersion condenser. In addition, the fluids travel along the double-pipe condenser in opposite directions, which may make the outlet temperature of water higher than the condensing temperature. A plate heat exchanger is also used as a condenser for the same purposes [19,23,36,51,52].

Although coaxial pipe condensers and plate condensers have higher heat transfer coefficients in comparison with condensers immersed in a storage tank, these condensers have higher flow resistances and need more power to pressurise the water that should flow at a certain speed. Since a thermosyphon heat exchanger induced a buoyancy force for the fluid natural circulation along the loop, a spiral condenser made of copper tube with a diameter of 6 mm was immersed inside a straight water pipe that was connected with a water storage tank [5,8,9]. Fig. 6 depicts the thermosyphon condenser used in an ISAHP. This configuration can promote the natural circulation of water as it absorbs heat released by the condensation of refrigerant vapour and then reduce the power consumption.

When a DX-SAHP is used to heat air directly, it usually uses an air-cooled heat exchanger with fin as its condenser to improve the thermal performance by increasing the heat transfer area [34,35,37,53].

3.5. Expansion valve

The expansion valve reduces the pressure of refrigerant in a DX-SAHP cycle and regulates its flow rate to adapt to the change in operating conditions. Both thermostatic and electronic types are widely used in DX-SAHP systems, as these expansion valves are effective on adjusting the flow rate of refrigerant to match the performance of compressors. It is noticeable that an electronic expansion valve is being favoured with the widespread use of variable frequency compressors. Part of the reason may be that the electronic one can control the superheat degree of a solar collector panel more accurately and steadily [12]. Furthermore, an electronic expansion valve with a controller combined with the variable speed compressor can obtain the high thermal performance and long-term reliability for the whole system by maintaining a perfect match between the heat pumping capacity of the compressor and the evaporative capacity of the collector-evaporator [12].

3.6. Refrigerants for DX-SAHP

3.6.1. Types of refrigerant

As a working fluid for SAHP systems, refrigerant must have high values of thermal conductivity, critical temperature and evaporation enthalpy to achieve good system performance, while must also have low values of freezing point, viscosity and specific volume capacity. Meanwhile, refrigerant must be environmentally friendly, cheap and safe. Fig. 7 presents a breakdown of refrigerants used in DX-SAHP systems in the published literature.

From the view of reducing GHG emissions, Aye et al. [54] reported that replacing R22 used in solar heat pump water heaters by environmentally friendly refrigerants, namely hydrocarbons, ammonia and carbon dioxide, can significantly reduce the direct global warming potential caused by the leakage and non-recovery of refrigerants. It makes sense to find more suitable refrigerants for DX-SAHP systems considering both for reducing the GHG emissions and for securing the stable and good system performance.

Chata et al. [55] investigated the effects of various refrigerants on

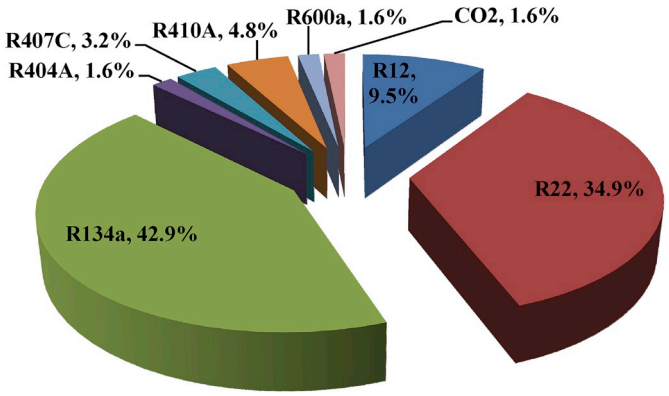

Fig. 7. Use percentage of assorted refrigerant in previous research works.

the thermal performance of a DX-SAHP system. In the same range of collector-evaporator temperature, the findings of this study showed that pure refrigerants (namely R-12, R-22 and R-134a) can achieve COP values at least 15% higher than those using refrigerant mixtures (namely R-404a, R-407c and R-410a). The results also pointed out that the system with R-12 produced the highest value of COP, followed by R-22 and R-134a. However, R-12 and R-22 have been banned or no longer produced to protect the ozone layer. Taking into account of the system thermal performance, R-134a is the most appropriate substitute for these banned refrigerants. The application of R-410a in DX-SAHP systems has increased in recent years [45,46]. The reason may be the nature of R-410a like zero ozone depletion potential and significantly lower condensation pressure drop than R-134a at the same mass flow rate [56]. Faria et al. [57] reported that the special thermodynamic and transport properties of CO_2 make the electronic expansion valve be a better choice for improving the COP for a transcritical DX-SAHP using CO_2 as the working fluid.

3.6.2. Charge amount of refrigerant

Besides the types of refrigerants, the charge amount of refrigerant is also an issue existing in the research area of DX-SAHP. In a research work conducted by Zhang et al. [14], the values of COP and collector efficiency increased by 36.7% and 42.3%, respectively, with the DX-SAHPWH getting a 50% refrigerant charge rise (from 1.2 to 1.8 kg). It is important to note that the more refrigerant a DX-SAHP has, the more harmful environmental impact refrigerant leaks will cause, if the refrigerant is not natural. Few works specially relate to deciding how much refrigerant to be charged for DX-SAHP systems, therefore, further theoretical and experimental research is needed, taking into account thermal performance and environmental effects.

3.7. Two-stage cycle system

The condensation temperature and the energy efficiency are closely related to the load temperature that is determined by the application of DX-SAHP. Since higher load temperatures result in higher condensation temperatures and more electricity consumption of compressor, the COP of DX-SAHP rapidly decreases. Therefore, the research of DX-SAHP systems on the single stage compression focused on the low temperature (below 60 °C) utilisation. With the intension of high temperature (60–90 °C) applications, Chaturvedi et al. [58] designed a two-stage DX-SAHP system (see Fig. 8) in which the low pressure stage cycle (LPSC) with a design condensation temperature of 50 °C and the high pressure stage cycle (HPSC) with a design condensation temperature of 90 °C, are coupled through a flash chamber. In the flash chamber, some of the liquid refrigerant from the HPSC expansion valve flashes off to the saturated vapour and mixes with the superheated refrigerant vapour from the LPSC compressor. Then the mixture is compressed by the HPSC compressor. Compared with a single-stage DX-SAHP, the two-stage DX-SAHP not only has better COP but also has larger values of collector efficiency at various condensing temperatures of 60, 70, 80 and 90 °C. For instance, the COP value is increased by more than 17%, while the solar collector efficiency is enhanced by more than two times, at the condensing temperature of 90 °C. This means that the two-stage DX-SAHP is favourable in high-temperature applications and has significantly better COP (i.e. lower operation cost) which may offset its additional initial investment cost. Further research is needed to assess its long-term economic benefit quantitatively.

4. Optimal design and operation of DX-SAHP

4.1. Optimal design of DX-SAHP

Whether the design is appropriate or not has a significant impact on the effective and stable operation of DX-SAHP. If the design is inappropriate, it may not achieve a good performance despite efforts made to control and operate the system with optimal strategies. Numerous studies have been carried out aiming to reveal rational design parameters of DX-SAHP systems.

4.1.1. Thermodynamic optimisation

Thermodynamic principles played a vital role in most of these research works. Finite-time thermodynamics (FTT) is a powerful tool for performance analyses and optimisation of real processes from a thermodynamic standpoint [58–60]. Torres-Reyes and De Gortari [61] performed a FTT analysis for performance optimisation of an irreversible DX-SAHP. The analytical expressions of maximum heating load and corresponding COP were developed to easily derive an optimal ratio between the condenser and collector-evaporator heat conductance ($x_{opt} = 1/2$) that makes the DX-SAHP have the optimal thermal performance. Shi [42] investigated the thermoeconomic optimisation of DX-SAHP further by using the FTT theory. Besides an optimal area ratio between the two heat exchangers, the analytical expressions of optimal evaporation and condensation temperatures were also deduced and given in Eq. (3) and Eq. (4), respectively, where, k_{Con} is the heat transfer coefficient of condenser, and K is the economical parameter that is the ratio of annual investment cost per unit heat conductance to annual cost per unit power.

$$T^*_{CE} = T_A + \frac{I_s(\tau\alpha)}{U_L} - \sqrt{\frac{K\,[T_A + I_s(\tau\alpha)/U_L]}{U_L F_R}} \tag{3}$$

$$T^*_{Con} = T_H\left\{1 - \frac{\sqrt{IU_L F_R K}}{\sqrt{k_{Con}U_L F_R\,[T_A + I_s(\tau\alpha)/U_L]} - \sqrt{Kk_{Con}}}\right\}^{-1} \tag{4}$$

The results showed that the ambient temperature, the heat loss coefficient of the collector and the heat-transfer coefficient of the condenser have little effect on the optimal thermoeconomic performance of the system.

From the literature, both the optimal design parameters and the optimal operating region for a real DX-SAHP system can be easily got by FTT for changeable meteorological, technical and economic conditions.

Exergy efficiency analysis was applied in optimising the design of DX-SAHP systems because it could quantitatively indicate which component should be paid more attention to and be modified [11,12,24,61,62]. For a DX-SAHP system, exergy efficiency is a key indicator that measures the ratio of the total exergy output (Ex_{out}) to the total exergy input (Ex_{in}) and is written as:

$$\psi = \frac{Ex_{out}}{Ex_{in}} = \frac{W_{Comp} + Ex_{rad} - I_{rr}}{W_{Comp} + Ex_{rad}} \tag{5}$$

where W_{Comp} is the input electrical power to the compressor, Ex_{rad} is the input exergy associated with incoming solar radiation and I_{rr} is the total exergy loss happening in all components of DX-SAHP. For instance, Li et al. [12] did exergy analyses for two different DX-SAHPWHs and

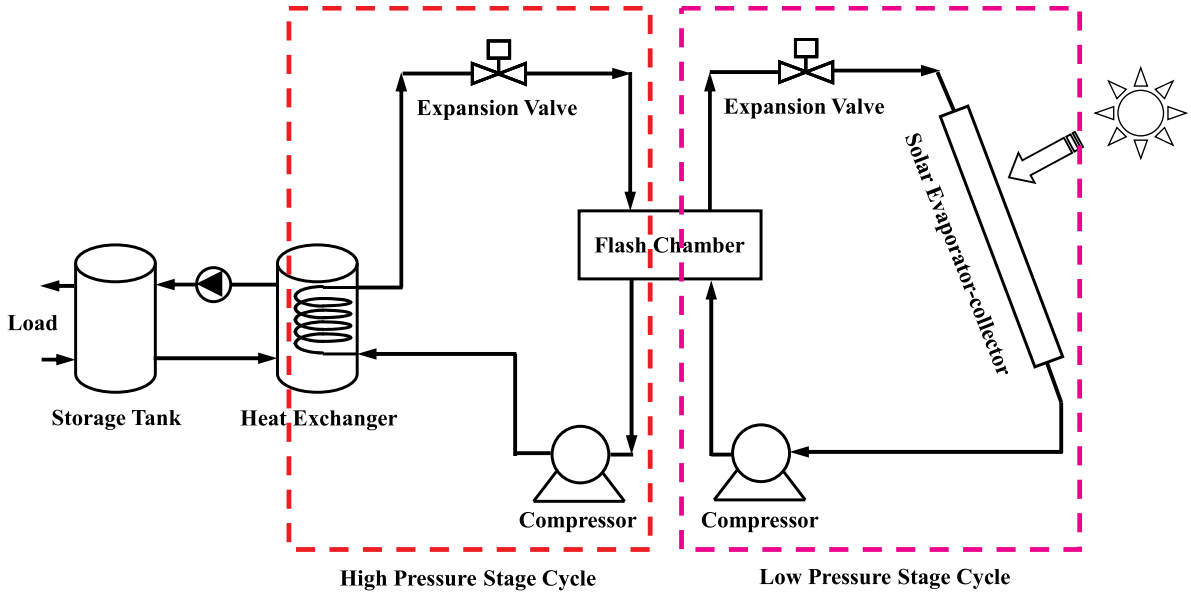

Fig. 8. Schematic diagram of two-stage DX-SAHP [58].

stated that the highest exergy loss occurred in the compressor (44.3% of I_{rr}), followed by the collector-evaporator (20.5% of I_{rr}), the condenser (9.9% of I_{rr}) and the expansion valve (4.4% of I_{rr}). The study also highlighted an optimal design methodology for the collector-evaporator based on the specific meteorological data in Shanghai and the assumption that the evaporation temperature was 5 °C lower than the ambient temperature. Obviously, a designer can get a better understanding of the quantitative inefficiency and the corresponding relative magnitude of each component by exergy efficiency analysis. However, exergy analysis was performed in very few of studies on water heating applications of DX-SAHP.

Scarpa et al. [63] developed a novel approach to investigate the design and performance of DX-SAHPWHs under steady working conditions using the second law of thermodynamics. It is important to note that the approach does not need to calculate refrigerant fluid thermodynamic properties and the optimisation goal (χ) can be a function of environmental parameters (G, T_e and T_{tap}) and design variables (T_u, $Mc/(UA\Delta t_m)$, $\alpha\tau/U$ and η_{II}) as shown in Eq. (6).

$$\chi = \frac{1}{T_u - T_{tap}}\left[1 - \varepsilon\left(\frac{\eta_b}{\eta_{el}} - 1\right)\right]\frac{(T_e + \alpha\tau G/U) - T_{tap}/(1+\varepsilon\eta_{II})}{Mc/(UA\Delta t_m) + (1+\varepsilon)/(1+\varepsilon\eta_{II})} \quad (6)$$

where, χ is saved primary energy index defined as the ratio of the actual saved primary energy of the DX-SAHP water heater to the primary energy consumed in the case of gas burner alone, T_u is the load temperature, T_{tap} is the tap water temperature, T_e is the ambient temperature, G is solar radiation, A is the active surface area of collector-evaporator, U is the overall heat transfer coefficient, Δt_m is the selected period, Mc is the thermal capacity of water, ε is the specific electrical energy consumption related to the compressor power, η_b is the combustion efficiency of gas burner, η_{el} is the conversion efficiency from primary-to-electric energy and η_{II} is the second law efficiency. The comparison between this approach and a detailed DX-SAHP dynamic model with high accuracy showed that there is a good agreement between the two techniques (errors always smaller than 8%) and the simplified method is adequate for predicting the overall behaviour of DX-SAHP with an auxiliary heat source. Apparently, the proposed approach can provide a comprehensive, simple, clear and practical guidance for the optimal design of DX-SAHPWHs under different potential operating conditions. Based on thermodynamic analyses, some researchers developed convenient graphical design methods for single-stage and two-stage DX-SAHP systems successively to suitably match the collector area with the compressor displacement capacity [55,58,64]. Each graphical design method needs one figure showing the variation of COP as a function of the collector temperature and the other figure showing the variation of collector efficiency as a function of the collector to ambient temperature difference at different solar radiation intensities as well as at various ratios of compressor displacement volume to collector area.

4.1.2. Numerical and experimental optimisation

A numerical or experimental method for factor analysis has been proven useful in determining optimal design parameters. Ye [37] applied two criteria, namely life cycle savings (LCS) and simple payback period (SPP), to identify the optimal solar evaporator-collector area with the best economic performance on basis of a simulation model of a multifunctional solar assisted heat pump system. The optimum collector area predicted by the SPP criterion (45 m^2) ignoring the cash flows was lower than that obtained from the LCS criterion (55 m^2). Hawlader et al. [33] developed a simulation model for a DX-SAHP water heating system using R-134a as the working fluid and validated it by experiments. The work reported that the thermal performance of DX-SAHP is mainly affected by compressor speed, collector area and volume of the heat storage tank. The findings of this study highlighted that the storage volume of 100 L m^{-2} collector area optimises the system performance in Singapore. The theoretical and experimental investigations done by Kuang et al. [65] showed clearly that the suitable ratio of storage volume to collector-evaporator area should be in the range of 75–125 L m^{-2} in consideration to a good technical-economic performance of DX-SAHP. When examining the component parameters on the system performance, Zhang et al. [14] drew a conclusion that the dimensions of the condenser pipe (length and internal diameter) have a remarkable influence on the thermal behaviour of DX-SAHP. There exists an optimum pipe length (70 m) and internal diameter (9 mm) to provide a maximum system COP.

4.2. Optimal control of DX-SAHP

Optimal control strategies are essential for an efficient operation of DX-SAHP systems. An accepted guideline is to control the refrigerant mass flow rate aiming to match with various load and weather conditions. The widespread use of variable speed compressors is the consequence of the requirement for controlling refrigerant flow rates.

Kuang et al. [36] further reported that jointly regulating refrigerant mass flow rates by a variable speed compressor and an electronic expansion valve with a controller can help a DX-SAHP work well under different weather conditions. Li et al. [12] demonstrated that the automatic control method combining the two controllable components (compressor and electronic expansion valve) effectively improves the thermal performance all year round. The research results showed that a DX-SAHPWH should work at or near solar noon while both solar radiation intensities and ambient temperatures have higher values for the better system performance [12,47]. Scarpa and Tagliafico [50] found that keeping the collector temperature lower than the ambient dew point temperature is another control method to improve the overall performance of a DX-SAHP system. The innovative work showed that the latent heat due to the condensation of moisture from air accounts for 20%–30% of the total thermal energy gained by the collector in the case of very low or no solar radiation and this method can help the DX-SAHP operate with an outstanding COP value of 5.8 in Genoa (Italy) having a moderate climate. Nevertheless, these are preliminary results and further invstigations are needed in different climatic regions to explore optimal collector temperatures throughout the year in view of dynamic control purpose.

5. Numerical simulation models

With the rapid development of computing technologies, researchers can conveniently analyse thermal performance, operation characteristics and impacts of various factors on performance by simulating mathematical models of DX-SAHPs.

5.1. Models for collector-evaporator

5.1.1. Models under different assumptions on fluid flow and heat transfer of refrigerant

As described before, a collector-evaporator is the important component bringing a lot of advantages to a DX-SAHP. The liquid-vapour phase change processes of refrigerant take place in this heat exchanger. In previous modelling research, there are three kinds of mathematical models for collector-evaporators.

The first one is called the simple model of flat plate collectors [47,66,67]. In this model, the small pressure drop through the collector-evaporator is neglected and the outlet refrigerant is assumed to be in the saturated vapour phase. Then the heat absorbed by the collector can be easily calculated by the single-phase fluid flow theory for the flat plate collector.

The second one is the homogeneous model based on the vapour-liquid two-phase flow theory [21,33,55,68–71]. This model takes into consideration the refrigerant pressure drop happening in the collector. In addition, it assumes that the liquid refrigerant and the vapour refrigerant are well mixed, so that the mixture is at thermal equilibrium and flows at the same speed. For this reason, the vapour-liquid mixture in the collector can be treated as a special fluid with specific properties.

The last one is the separated flow model for the two-phase mixture [17,19,42,72]. In this model, the whole collector-evaporator is dynamically subdivided into a two-phase region, a superheated region and/or a supercooled liquid region along the evaporator tube. Different fluid flow and heat transfer theories are used in different phase regions. Both the lumped parameter approach and the distributed parameter method can be applied in each region. The model results are better fit with the actual fluid flow and heat transfer of refrigerant in the collector. However, the convergence of its numerical solution takes more computing time than those of the former two models.

5.1.2. One-or two-dimensional models

The comparison between one-dimensional and two-dimensional mathematical models of unglazed collector-evaporator was made in Ye's analytical investigation [37]. The simulation results using the two different models had less than 4.2% of average relative difference. Additionally , the 1-D model is simpler than 2-D model, which helps to shorten computing time. These are reasons why the vast majority of simulation research adopted the 1-D model of collector-evaporator.

5.1.3. Models under humid air condensation or frost conditions

A collector-evaporator is a heat exchanger filled with refrigerant and contacts directly with ambient air. If an evaporation temperature is less than the environmental dew point temperature, a portion of the moisture of ambient air will be condensed on the collector-evaporator surface during the operation. The condensed water will be frozen if the temperature is below 0 °C. Heat transfer performance influenced by the condensation or the ice formation should be taken into account in a model of collector-evaporator for its optimal design and operation. But, there are only a few investigations on the effects of condensation or frost phenomenon on the collector performance. Based on the mass transfer theory, Morrison [47] developed an expression of the latent heat from condensation processes that is related to the collector efficiency coefficient and the water vapour partial pressure difference between ambient air and the water film on the surface. The performance evaluation indicated that when a packaged DX-SAHPWH worked in Sydney under warm temperate coastal climate conditions and was controlled by a strategy keeping its compressor running throughout the day, the thermal energy from condensation/rain accounted for about 18% of the total daily energy intake by its collector-evaporator. Facão et al. [41] also used this expression to improve their collector-evaporator model. Ye [37] took into account the condensation effect by introducing a condensation heat-transfer coefficient in the collector-evaporator model. Applying the heat and mass transfer theories, Scarpa and Tagliafico [50] concluded that when condensation takes place, higher relative humidity will lead to a higher energy gain from ambient air and a better thermal performance of the collector. A mathematical model derived by Moreno-Rodríguez et al. [51,52] can be used to calculate the latent heat of frost to evaporate the refrigerant in a collector-evaporator when considering the thermal resistance of the frost layer on the collector surface. Further research is needed in cold climate regions to develop a comprehensive dynamic heat-transfer model considering both the frost formation and the refrigerant boiling in the collector-evaporator.

5.2. Models for the whole system

Previous simulation models of DX-SAHPs can be broadly classified into lumped parameter models [7–9,12,33,36,46,47,73–75] and distributed parameter models [22,42,57,76]. Steady lumped parameter models have been adopted for compressors that reach steady state faster than evaporators and condensers. In distributed parameter models, both the collector-evaporator and the condenser are divided into numerous infinitesimal elements along the refrigerant flow direction, and local heat transfer coefficients as well as friction coefficients are applied to the energy and the momentum equations for each control element, respectively. It leads to a high degree of accuracy, with additional model complexity and complex calculations. Hence, researchers may prefer to use the lumped parameter approach that has less computation time and meets precision requirements for numerical analyses of DX-SAHPs.

6. Traditional and novel applications

6.1. Water heater

Researchers have conducted numerous investigations on DX-SAHPs for water heating in recent decades [77]. DX-SAHPWHs provide hot water not only for household use, but also for commercial use, such as bathhouses and large buildings. Tables 1 and 2 show that hot water load temperatures were not more than 60 °C in almost all research

Table 1
Overview of researches on DX-SAHPWH in the US, Europe and Oceania.

Reference	Refrigerant	T_{water} (°C)	COP (−)	Collector (m^2)	Compressor	Condenser
Canada, 1983 [78]	R-12	40, 60 (T_{Con})	> 2.5	1.72, with removable single glazing and back insulator	open type 675 rpm	series air & water cooled
US, 1984 [4]	R-12	40-50 (T_{Con})	2–3	3.39, with back insulator	open type 0.0000832 m^3/s	–
US, 1987 [79]	R-12, R-22	50	3.5 (R12) 2.7 (R22)	2.0, bare flat plate	variable capacity 262–1725 rpm	shell-tube
US, 1998 [80]	R-12	~30	2.5–4.0	3.48, bare flat plate	variable capacity 0.0007036 m^3/s	shell-tube
US, 2014 [81]	R-134a	60	4.0–5.6	3.0, with single cover	0.0003518 m^3/s	–
US, 2016 [82]	R-134a	50, 60 (T_{Con})	3.6–5.6	40, -	0.005304 m^3/s	–
Italy, 2010 [23]	R-22	55	4.5–8.4	7.2, PV/T, removable glazing and back insulator	scroll type 1650 W	plate type
Italy, 2011 [7]	–	45	~8.0	2.0, bare flat plate	variable capacity 1600–4500 rpm	immersion
Italy, 2016 [50]	R-134a, R-600a	45 (T_{Con})	5.8	1.0, bare flat plate	variable capacity	tube-in-tube
ESP, 2012 [40]	R-134a	55	2.2–4.3	1.6, bare flat plate	rotary type 390–550 W	immersion
ESP, 2012 [51]	R-134a	51	~2.2	5.6, bare flat plate	1100 W	plate type
Poland, 2014 [41]	R-134a	50	–	1.6, bare flat plate	455 W	immersion
Greek, 1998 [61]	R-12	47–55	> 3.0	2, bare	350 W	immersion
Australia, 1994 [47]	–	–	2.4–4.2	-, unglazed roll-bond	rotary type	wrap-around
Australia, 2002 [54]	R-22	60	–	~6, -	1100 W	–
Australia, 2007 [48]	R-22	56	5-7 (day) 3-5 (night)	4, unglazed roll-bond	800 W	wrap-around

projects, which is because the recommended designed value of condensing temperature shall not exceed 60 °C for achieving high system performance [12,47,73,84]. There may be three main reasons for the increase in low-temperature water heating applications. Firstly, it can be observed from Tables 1 and 2 that DX-SAHPWHs have satisfactory thermal performance in both warm and cold climates. Secondly, the low cost and high energy-saving benefits of hot-water production are outstanding advantages of DX-SAHPWHs. Aye et al. [54] found that the electricity consumption of DX-SAHPWH was between 0.011 and 0.015 kWh L^{-1} of hot water at 60 °C in eight Australian cities and it was much less than the electricity consumption of an air-source heat pump water heater. For a DX-SAHPWH in Taipei, the average electricity consumption per litre of hot water at 57 °C was 0.019 kWh that was only a third as much as a conventional electric water heater [6]. Yang [49] performed an economic analysis for an oil-fired water heater, a gas-fired water heater, an electric water heater, a solar water heater and a DX-SAHPWH, and reported that the DX-SAHPWH was the most economical and competitive alternative as its electricity consumption per litre of hot water at 45 °C was only 0.0145 kWh. The economic studies conducted by Hawlader et al. [33] showed that the minimum simple payback period of the DX-SAHPWH was just about two years. Additionally, the DX-SAHPWH has obvious advantages in reducing GHG emissions compared with the air-source heat pump (for example, in Melbourne, the DX-SAHPWH capable of heating 270 L of water from 20 to 60 °C cuts carbon dioxide emissions by up to about 5 tonnes over its lifetime of 15 years), and is mostly competitive in the climate flexibility in comparison with the thermosyphon solar water heater [54]. In another study, Fernández-Seara et al. [40] conducted a series of interesting experiments in a climate chamber with an air temperature range of 7–22 °C and a constant relative humidity of 55%, to assess the performance of DX-SAHPWH under zero solar radiation conditions. It can be concluded from these experiments that the DX-SAHPWH can make good use of ambient air as its heat source and obtain the remarkable performance even there is no solar radiation.

Both split-type and integral-type DX-SAHPWHs have achieved commercial success since 1990s. As illustrated in Fig. 9, ISAHP with an aesthetic appearance has been commercially available as a domestic hot water heater due to its clean, efficient, and energy-saving nature.

6.2. Space heating

Since 1980s, the application of DX-SAHPs to space heating has made great progress, as a result of the global energy dilemma and the environmental degradation. Based on the reviewed articles, Fig. 10 briefly presents the types of DX-SAHP space-heating systems. It is apparent that the fan-coil unit and the floor radiation heating unit are the two major terminal unit types on which previous research has focused. This is mainly owing to the fact that DX-SAHPs can generate low-temperature hot water effectively. In term of different working fluids for an indoor heating unit, DX-SAHP systems can be subdivided into the refrigerant/air heat convection design [11,53,61,78,88], the water/air heat convection design [52], the radiant floor heating with water design [45] and the radiant floor heating with refrigerant design [89].

Krakow and Lin carried out one of early studies and focused on the operation performance of DX-SAHPs for space heating in cold climates [78]. The study showed that the system had a minimum COP value of 2.6 even in bad weather conditions (ambient temperature, −23 °C, and horizontal global solar radiation intensity, 200 W m^{-2}) and demonstrated that a glazed flat-plate collector was a better fit than an unglazed solar collector in cold regions. Other researchers have also contributed to the development of this technology.

Ooi [53] also tested the operating characteristics of a DX-SAHP with an electric resistance heater for spacing heating in Canada. As shown in Table 3, the system COP during the night-time without solar radiation varied from 1.4 to 2.3 for different ambient temperatures. Ooi stated that if there was no limitation of a maximum refrigerant flow rate of 0.016 kg s^{-1}, the system would keep a constant indoor temperature of 21 °C with higher COP values. Also, the heating cost of the DX-SAHP space-heating system (Can$ 8.93 GJ^{-1}) had a saving of over 9% compared with that of the conventional heat pump heating system (Can$ 9.82 GJ^{-1}).

Thousands of high-rise buildings are springing up in modern cities. Generally, exterior walls of these buildings have the restricted installation space in the perpendicular direction for domestic solar or air source heat pumps bulky configurations. In addition, the ducting layout of heat pump systems for space heating is another challenge. Therefore, Dong [89] proposed and investigated a solar integrated air source heat pump system aiming to meet the individual space-heating demand of users living in high-rise apartment buildings. The schematic diagram

Table 2
Overview of researches on DX-SAHPWH in Asia.

Climate region	Year/Authors	Refrigerant/Load temperature	System components	COP
JPN	1999 [73] Ito et al.	R-12 30, 40, 60 °C (T_{Con})	Collector: bare flat plate, 3.24 m^2 Compressor: rotary type, 350 W Condenser: wrap-around	2.2–5.8 (winter)
JPN	1999 [83] Hulin et al.	– 65 °C	Collector: aluminium fin tubes	2.7–3.7
SIN	2001 [33] Hawlader et al.	R-134a 30–50 °C	Collector: unglazed plate with black paint and back insulation, 3 m^2 Compressor: open type, variable capacity Condenser: immersion Thermostatic expansion valve Storage tank: 250 L	4–9
CHN	2003 [17] 2004 [65] 2005 [84] Kuang et al.	R-22 [17] R-134a [65,84] 50 °C	Collector: bare flat plate, 2 m^2 [17], 1 m^2 [65], 1.05 m^2 [84] Compressor: piston, 249 W [17], 215 W [65,84] Condenser: immersion, 5 m^2 Thermostatic expansion valve Storage tank: 150 L [17], 140 L [65,84]	4-6 [17] 3.1 average [65] 4.18 average [84]
CHN	2006 [18] Xu et al.	R-22 55 °C	Collector: flat-plate type with spiral-finned tubes, 2.2 m^2 Compressor: rotary type, 400 W Condenser: tube-in-tube Storage tank: 150 L	3.98–4.32
CHN	2006 [19] Pei 2008 [21] Ji et al.	R-22 55 °C [19] 30 °C [21]	Collector: PV/T type with glass cover and back insulation, 5.49 m^2 Compressor: variable capacity, 795 W Condenser: plate type Electronic expansion valve	6.3 average [19] 3.8–8.4 [21]
CHN	2007 [12,85] Li et al. 2011 [39] Kong et al.	R-22 50 °C	Collector: unglazed flat plate with paint coating, 4.20 m^2 (A prototype); copper sheet with black paint coating, 2.08 m^2 (B prototype) Compressor: rotary type, 750 W (A), 400 W (B) Condenser: immersion, 1.72 m^2 (A), 1.44 m^2 (B) Thermostatic expansion valve Storage tank: 150 L	5.21-6.61 (spring, A) 4.13-5.12 (autumn, B)
CHN	2007 [49] Yang et al.	R-22 45 °C	Collector: unglazed flat plate with black paint coating, 17 m^2 Compressor: scroll type, 1650 W Condenser: tube-in-tube Thermostatic expansion valve Storage tank: 1200 L	3.5–5.1
CHN	2011 [26] Wei et al. 2011 [27] Wu et al.	R-22 50 °C	Collector: all-glass evacuated tube with refrigerant copper tube and PCM (paraffin [26], decanoic acid [27]) Compressor: variable capacity, 735 W Condenser: tube-in-tube Electronic expansion valve Storage tank: 150 L	5.63 (sunny day), 4.13 (rainy day), 4.24 (night) [26] 7.56 [27]
CHN	2012 [86] Xu et al.	R-134a 60 °C	Collector: PV/T type, 1.28 m^2 Condenser: tube-in-tube Storage tank: 180 L	3.8
CHN	2012 [24] Fu et al.	R-134a 46.8–54.1 °C	Collector: Heat-pipe PV/T type with back insulation, 4.668 m^2 Condenser: immersion Storage tank: 560 L	3.32–4.01
CHN	2014 [14] Zhang et al.	R-22 50 °C	Collector: unglazed flat plate, 4.2 m^2 Compressor: 2830 rpm Condenser: immersion Thermostatic expansion valve Storage tank: 150 L	3.7–5.5
CHN	2014 [15] 2015 [43] Sun et al.	R-134a 55 °C	Collector: bare roll-bond, 2 m^2 Compressor: reciprocating, 8.8 cm^3/rev Condenser: immersion Thermostatic expansion valve Storage tank: 150 L	3.9–5.5
CHN	2016 [44] Deng et al.	R-134a 55 °C	Collector: parallel flat plate & finned-tube, 2m^2 Compressor: 2980 rpm Condenser: immersion Electronic expansion valve Storage tank: 150 L	> 4
CHN	2017 [46] Kong et al.	R-410a 50 °C	Collector: bare flat plate, 4.2 m^2 Compressor: rotary-type, 750 W Condenser: immersion Electronic expansion valve Storage tank: 150 L	3.6–3.9
TPE	1999 [5] 2001 [8] 2003 [6,9] Huang et al. [5,6,8] Chyng et al.	R-134a 52 °C [5] 61–68 °C [8] 57 °C [6] 57.2 °C [9]	Collector: unglazed tube-in-sheet, 1.44 m^2 [5,6,8], 1.86 m^2 [9] Compressor: reciprocating, 150 W [5], 250 W [6,8,9] Condenser: thermosyphon Storage tank: 120 L [5], 105 L [6,8,9]	2.54 [5] 2.5-3.7 [8] 1.7-2.5 [9]

(*continued on next page*)

Table 2 (*continued*)

Climate region	Year/Authors	Refrigerant/Load temperature	System components	COP
TPE	2005 [16] Huang et al.	R-134a 55 °C	Collector: unglazed circular-shape heat pipe, 3.78 m^2 Compressor: reciprocating, 550 W Condenser: immersion, 0.62 m^2 Capillary tube Storage tank: 240 L	3.32
TPE	2007 [74] Huang et al.	R-134a 55 °C	Collector: unglazed tube-in-sheet (I, II model), heat-pipe (III model) Compressor: reciprocating, 150 W (I), 250 W (II), 600 W (III) Storage tank: 115 L (I), 130 L (II), 240 L (III)	2.12 (I) 1.85 (II) 2.24 (III)
HKG	2009 [87] Li et al.	– 55 °C	Collector: 6 m^2 Storage tank: 280 L	4
HKG	2010 [38] Chow et al.	R-134a 50 °C	Collector: bare flat plate with back insulation, 12 m^2 Compressor: reciprocating, variable capacity, 1 kW Condenser: immersion Capillary tube Storage tank: 2500 L	6.46

Fig. 9. Shape of commercialized ISAHP [74].

and the evaporator prototype of the first-generation system are provided in Fig. 11. In this system, a solar finned tube heat exchanger with a selective paint coating on surface acts as the collector-evaporator collecting heat from both solar and ambient air energy, while a capillary copper pipe network is used as the condenser as well as the floor-heating unit, which makes the refrigerant in the pipe network vapour directly release heat to indoor air. So, the space-heating system had a maximum COP value of 3.99 in winter in the city of Taiyuan, China.

6.3. Desalination

Since Hawlader et al. [90] coupled a DX-SAHP with a seawater desalination system, a number of theoretical and experimental works have been done in Singapore and published in the literature such as [91–94]. In such desalination systems, the DX-SAHP has a cooling copper coil evaporator installed in parallel with a solar collector-evaporator collecting ambient energy. The cooling coil evaporator is mounted on the top of the desalination chamber in order to condense the distilled vapour into fresh water that is easy to be collected. The condenser installed on the bottom of the chamber is designed to give thermal energy for the evaporation of the feed water. The overall findings of the experimental studies conducted by Amin et al. [94] remarked that the desalination system using DX-SAHP achieved excellent COP values of 4.33–10.78 and 5.69–10.43 at different compressor speeds of 1500 rpm and 1800 rpm, respectively. In another study, Amin et al. [93] reported that the SAHP desalination system with a 67 m^2 collector-evaporator used to produce 900 L of fresh water every day had a short simple payback period of less than 3.5 years.

6.4. Vaporisation of liquid fuels

Some gas fuels, such as petroleum gas and natural gas, have a remarkable economic value and a convenience for storage and transmission after being liquefied [95]. Combustion of these fuels can reduce the emissions of air pollutants as well as the environmental costs in comparison with oil and coal. Hence, LPG (liquefied petroleum gas) and LNG are widely used as green transition fuels in global industrial, commercial and residential applications. LPG and LNG have to be vaporised into gas phase before being used as fuels by terminal users.

However, the vaporisation of LPG is an energy intensive process which energy consumption is about 127 kWh t^{-1} [42]. Shi [42] proposed a new LPG vaporisation system utilizing solar assisted heat pump (abbreviated as DX-SAHPV), in order to reduce fossil fuel or electricity consumption for the traditional vaporisation process and broaden the application fields of the DX-SAHP technology. As shown in Fig. 12, the DX-SAHPV system mainly consists of a DX-SAHP, a thermal storage tank, an instantaneous gas-fired water heater as an auxiliary heat source, and a vaporiser. R-417a absorbs solar and air energy in a bare flat-plate collector with a total area of 12.78 m^2 and heats the water within the storage water tank after being compressed by a WHP09800DCV compressor with a capacity of 2415 W. Hot water passes through the vaporiser and evaporates liquid LPG into vapour. The water temperatures of 55 °C and 45 °C in the water tank control the stop and start of the DX-SAHP, respectively. In terms of the nature of LPG spontaneous vaporisation (SV) and the fluctuations both of residential gas load and of meteorological conditions, six different operation modes can be realized with the on/off of the compressor, the water pump and valves. Table 4 details these modes and their corresponding operating conditions. Table 5 shows the monthly performance of the DX-SAHP in this LPG vaporisation system that is designed for a 1000-family community in Beijing. It can be concluded that this new LPG vaporisation system can not only take advantage of both solar and ambient air energy, but also help to realise the stable heat production of DX-SAHP throughout the year.

An LNG vaporisation system by using DX-SAHP [31], designed to produce warm air to prevent frost formation on the surface of a LNG ambient air vaporiser and increase its heat-transfer performance, is illustrated schematically in Fig. 13. As seen from this figure, the design introducing LNG into a collector-evaporator can realise the control of optimal panel temperature that is lower than the ambient temperature. This makes the DX-SAHP collect heat from ambient air effectively even

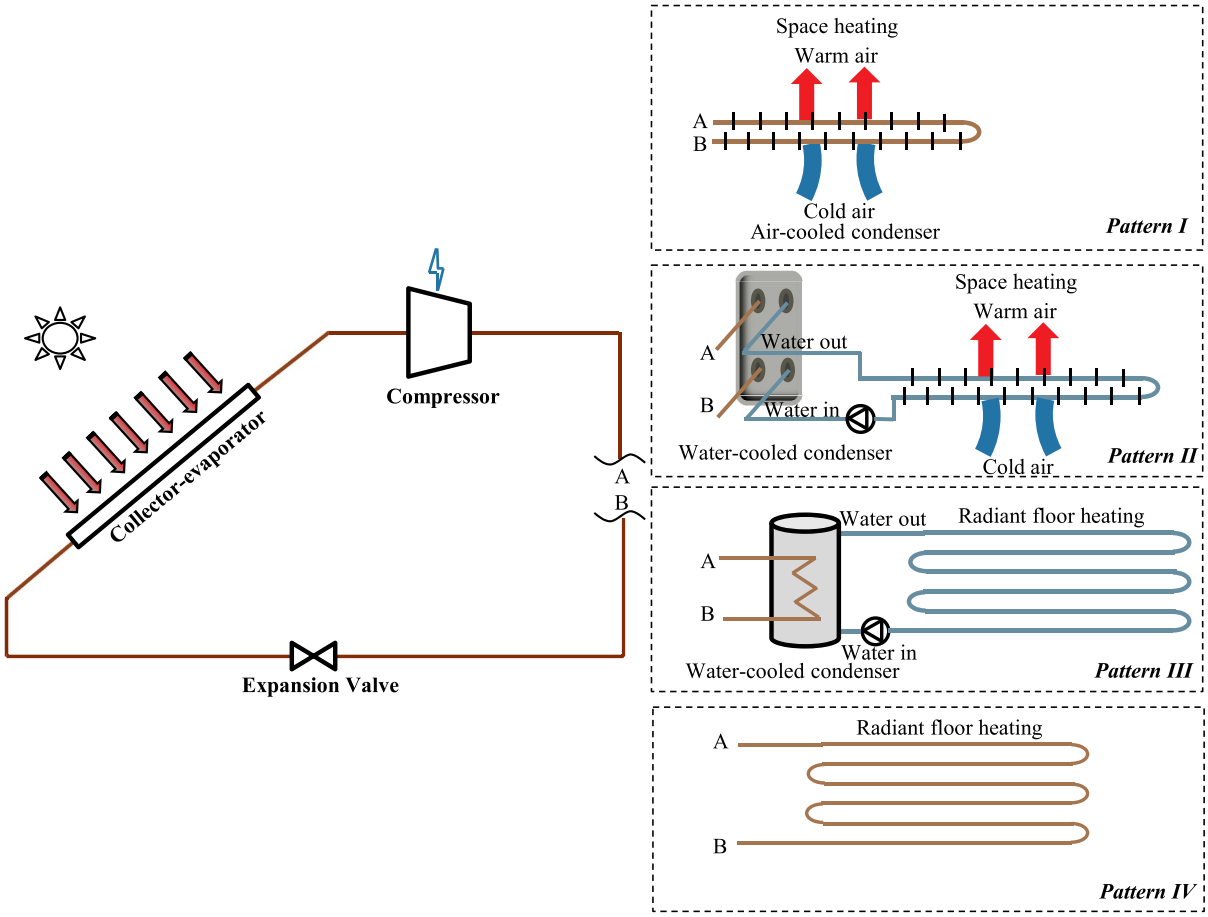

Fig. 10. Commonly used DX-SAHP space-heating systems.

Table 3
COP of the DX-SAHP space heating system during the period of Sep 86 - Mar 87 in Ref. [53].

Maximum COP		Minimum COP	Average COP		
day	night	night	total	day	night
2.6	2.3	1.4	2.0	2.1	1.8

during night time. After being propelled by a fan and heated by a condenser, the warm air transfers heat to the ambient air vaporiser to vaporise cryogenic LNG. Further theoretical and experimental research is needed to explore the operation characteristics and the potential benefits of DX-SAHP for LNG vaporisation applications.

6.5. Multifunctional applications

Expanding the functionality of DX-SAHP systems is a better option to maximise their usage, reduce operation cost and make the best use of available solar energy. A few of previous works have focused on the design, simulation and experimental test of DX-SAHPs to estimate the performance and the technical feasibility for multifunctional applications [34–37,78,92,96,97]. As early as 1980s, Morgan [96] reported the theoretical and experimental work on a DX-SAHP system for air-conditioning and water heating in tropical climates while Krakow et al. [78] investigated the thermal performance of an experimental DX-SAHP system for hot-water production and space heating in cold climates. The multifunctional DX-SAHP systems are summarised and discussed in Table 6 with a focus on functionality, system features,

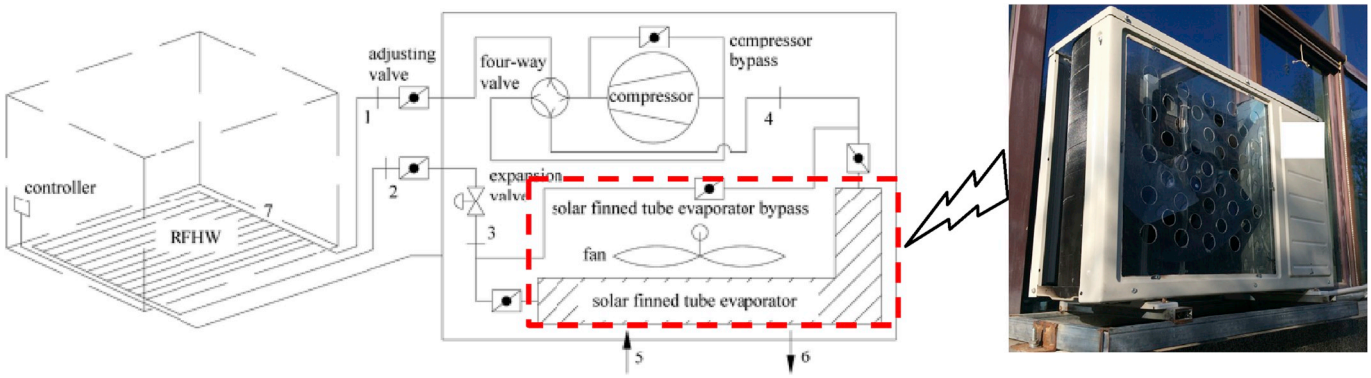

Fig. 11. Solar integrated air source heat pump for radiant floor heating without water [89].

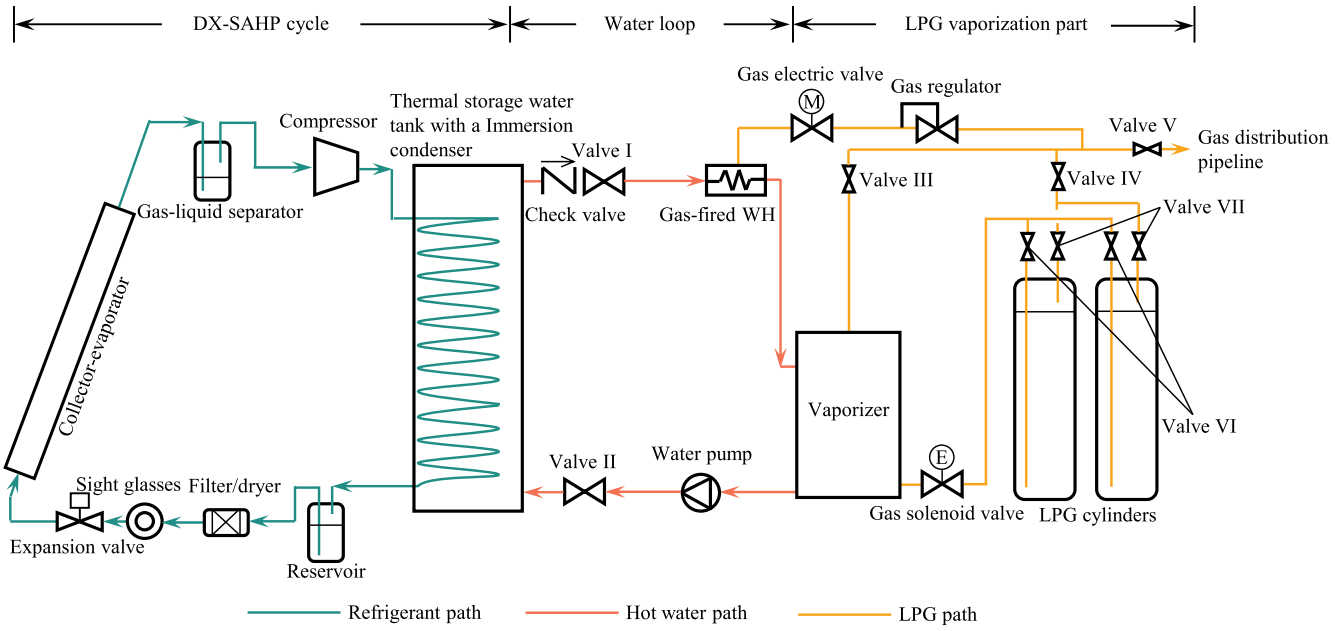

Fig. 12. Schematic diagram of DX-SAHPV system [42].

operation states and results of these research projects.

Hawlader et al. [34,35] simulated and tested a SAHP dryer and water heater in February in Singapore. The SMER (specific moisture extraction rate) is defined for this system by the ratio of the moisture content removed from the product to the total energy input. The findings indicated that the SMER was significantly affected by the weight of green beans being dried and the value was 0.65 kg kWh^{-1} for 20 kg of products. The SMER is also influenced by air mass flow rates and further research is needed to investigate an optimal flow rate for a high value of SMER. The studies concluded that the COP for the system will reduce with the decrease in latent heat recovery from the drying product as the drying process progresses.

Ye [37] further designed a multi-function SAHP system able to cool the indoor air while recovering the heat from condensers to heat the water and the air for drying purposes. Table 7 summarises the measured COP values under the five different operation modes in a typical day in Singapore. With reference to Table 7, the innovative system has good thermodynamic performance no matter which mode it runs in. The investigation also demonstrated that the system payback period first decreases significantly and then increases gradually with increasing solar collector area. In other words, there is an optimal collector area for the minimum payback period. This is because the increase of collector area before reaching the optimum value causes much more fuel savings than the cost increase. The economic analysis of the system for a hotel with the room area of 600 m^2 reveals that it has a strong market potential with a minimum payback period of 1.5 years.

Kuang and Wang [36] reported the long-term performance of a three-in-one DX-SAHP system designed for space cooling in summer, space heating in winter and water heating during the whole year. The experimental results obtained in the first half of 2004 in Shanghai, China, testified that the system running in the space-heating-only mode maintained the daily-averaged indoor temperature in the range of 16.7–19.1 °C with acceptable COP values varying from 2.1 to 2.7. In the water-heating-only mode, it produced 200 L of water at 50 °C in a short time (no more than 3 h) under different weather conditions. In the space-cooling-only mode, the compressor only operated at night to make full use of off-peak electric power by cooling the water in the heat storage tank for the daytime space-cooling and the system had an

Table 4
Operation modes of DX-SAHPV and their operating conditions.

	Brief description of mode	Operating conditions
Mode 1	SV Compressor, water pump, gas solenoid valve and Valve III off; Valves IV − VII on	When gas load is low and the water temperature in the storage tank is larger than 45 °C, the SV of LPG in the cylinders is adequate to meet the gas demand of users.
Mode 2	SV + heat charging Water pump, gas solenoid valve and Valve III off; compressor and Valves IV − VII on	When gas load is low, but the water temperature in the storage tank is less than 45 °C, the SV of LPG in the cylinders is adequate to meet the gas demand and the operation of the DX-SAHP heats the water in the tank.
Mode 3	SV + water heated vaporisation Compressor off; water pump, gas solenoid valve and Valves III − VII on	When gas load goes over the SV capacity of LPG in the cylinder and the water temperature in the tank is larger than 45 °C, hot water in the tank passes through the vaporiser and vaporizes rest amount of liquid LPG to meet the gas demand of users.
Mode 4	SV + water heated vaporisation + heat charging Compressor, water pump, gas solenoid valve and Valves III − VII on	When gas load goes over the SV capacity of LPG in the cylinder and the water temperature in the tank is less than 45 °C, the DX-SAHP runs to heat the water in the tank that vaporizes LPG to meet the gas demand.
Mode 5	SV + water heated vaporisation + auxiliary heating Compressor off; gas-fired WH, water pump, gas solenoid valve and Valves III − VII on	When gas load is very large, hot water cannot give enough heat to vaporise required demand of LPG, and the water temperature in the tank is larger than 45 °C, the instantaneous gas burner heats the hot water further to meet the LPG vaporisation demand.
Mode 6	SV + water heated vaporisation + auxiliary heating + heat charging Compressor, gas-fired WH, water pump, gas solenoid valve and Valves III − VII on	When gas load is very large, hot water can no longer support the full heating load, and the water temperature in the tank is less than 45 °C, the instantaneous gas burner heats the hot water further to meet the LPG vaporisation demand. Simultaneously, the DX-SAHP delivers heat to the water in the tank.

Table 5
Annual performance of the heat pump in the DX-SAHPV system in Ref. [42].

Month	Average ambient temperature (°C)	Average solar radiation (MJ m^{-2})	Average evaporation temperature (°C)	Average condensing temperature (°C)	Average heat capacity (kWh)	Average collector efficiency	Average COP
Jan	−3.80	253.40	−4.82	56.50	810.46	0.97	2.75
Feb	−1.60	336.30	−1.94	57.34	926.91	0.92	2.89
Mar	7.70	463.60	1.25	58.29	880.74	1.06	3.03
Apr	14.40	542.50	6.35	59.60	820.94	1.06	3.29
May	19.40	594.50	7.16	59.58	886.65	1.18	3.34
Jun	24.50	567.10	8.10	59.94	908.37	1.33	3.36
Jul	26.50	531.40	6.33	59.43	854.62	1.54	3.30
Aug	25.60	513.60	8.61	59.97	847.74	1.29	3.40
Sep	20.40	400.80	5.12	59.18	795.45	1.37	3.22
Oct	12.90	357.80	2.25	58.62	795.01	1.24	3.08
Nov	5.40	263.80	0.68	58.17	798.63	1.14	2.95
Dec	−0.50	217.30	−4.08	57.25	784.07	1.15	2.74

average COP value of about 2.9. As highlighted in this study, the multi-function capability explains the high utilisation rate of this system with low operation cost throughout the year.

7. Conclusions

A comprehensive review on the recent status of DX-SAHP systems has been extensively and critically studied. The key conclusions are listed as follows:

(1) The power energy consumed to drive a DX-SAHP is only about 30% of the total transferred energy [98] as it integrates the solar thermal technology with the heat pump. Therefore, the DX-SAHP technology conserves fossil fuels like coal, oil and natural gas, and results in a reduction of GHG emissions from non-renewable energy consumption. As illustrated in Ref. [99], the solar assisted heat pump systems can yield an annual GHG emission reduction by 19% (12.59 Mt of CO_2 equivalent per year) in the Canadian residential sector.
(2) Although it is still in the research and development stage, the proper integration of DX-SAHP and some advanced technologies, such as solar photovoltaic technology, PCM thermal storage technology and heat pipe technology, has the potential to achieve high COP values under various weather conditions.
(3) The DX-SAHP water heaters are ideal for domestic hot water production due to both economical and energy-saving advantages compared to conventional water heaters. Some of the research covered in this review shows that the typical range of electricity consumption for DX-SAHPWHs is about 0.01–0.012 kWh L^{-1} of low-temperature hot water at 45–60 °C.
(4) Even though its market share is extremely small, the DX-SAHP technology is gaining more attention with its novel utilisation in various industries.

8. Further recommendations

Although huge efforts and important progress have been made until now, further investigations listed as following are still needed to promote the market penetration of the technology.

(1) *Developing high efficient, low-cost and building-integrated collector-evaporators.* A collector-evaporator is a key component that affects the thermal performance of DX-SAHP. Past theoretical and experimental investigations have proved that new types of collector-evaporators (i.e. PV/T evaporators, collection/energy storage/evaporation evaporators with PCM, etc.) are beneficial to the best and efficient use of solar energy. However, high cost is the bottleneck for their marketisation. An economic analysis showed that the simple payback period of a heat pump with heat-pipe PV/T collector was as long as 14 years [24]. Although having achieved commercial successes since the early 1990s, DX-SAHPWHs are not universal and do not gain more public acceptance yet, especially in modern cities of high-rise apartments. One reason may be that current unglazed bare flat-plate collectors are not aesthetically appealing for the exteriors of buildings. Moreover, dew condensation on the surface of collectors would lead to damage of external walls of high-rise buildings. Further works on collector-evaporators are essential to address a trade-off among performance, cost and aesthetic design.
(2) *Establishing standardization guideline for the design, the component*

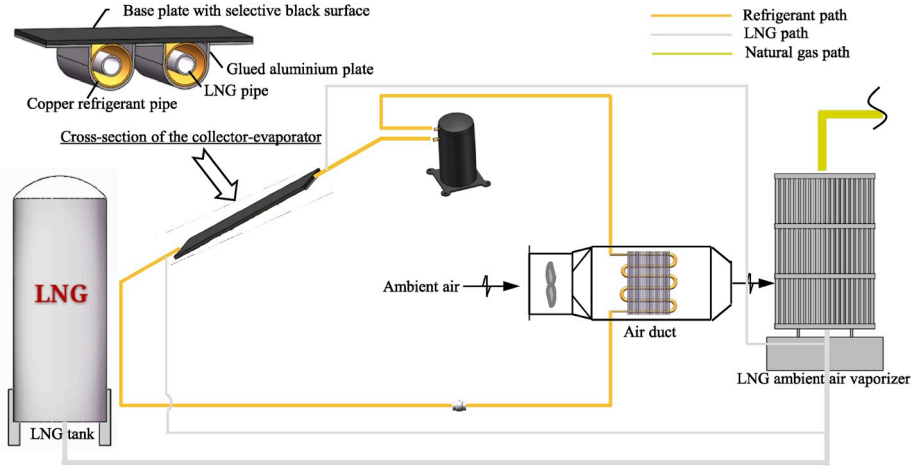

Fig. 13. Schematic diagram of an LNG vaporisation system utilizing DX-SAHP [31].

Table 6
Summary of DX-SAHP systems for multifunctional applications.

Reference	Functionality	System features	Operation states	Research methods	Results
[34,35]	Water heating + drying	Two parallel evaporators with individual expansion valves, two condensers (an air condenser and a water-cooled condenser) in series	A collector-evaporator absorbs thermal energy from solar radiation and/or ambient air, a solar air collector recovers both latent and sensible heat from the exit air from the dryer	Simulation + experiments	System: maximum COP = 7.0 at a drying temperature 55 °C and an air mass flow rate 0.06 kg s^{-1} Capacity: moisture extraction rate 0.65 kg kWh^{-1} (20 kg green beans), water temperature 54 °C Collector-evaporator: maximum efficiency 86% Solar air collector: maximum efficiency 70%
[90]	Water heating + desalination	A collector-evaporator, two condensers in series, a desalination with a cooling coil evaporator	A coil condenser for seawater desalination, an immersion condenser for water heating	Theoretical analysis + experiments	System: COP = 5.0–7.0 Collector-evaporator: maximum efficiency 88.4%
[92]	Water heating + desalination + drying + space cooling	Three evaporators in parallel, two condensers in parallel	A collector-evaporator collects heat from solar radiation and/or ambient air, a room evaporator for air conditioning, copper coil evaporator for distilled water	Theoretical analysis + experiments	System: maximum COP = 5.8 Capacity: maximum fresh water output 9.6 L h^{-1} in the multifunction mode, maximum fresh water output 30 L h^{-1}
[37]	Water heating + drying + space cooling	A collector-evaporator and a room evaporator in parallel, an air-cooled condenser and a water-cooled condenser in series, each condenser and a bypass line in parallel	Five operating modes: full mode, no water condenser (NoWC) mode, no air condenser (NoAC) mode, no room evaporator (NoRE) mode, no evaporator-collector (NoEC) mode	Simulation + experiments	System: monthly COP varies 4.75-4.85 Collector: monthly efficiency varies 1.5-1.9
[36]	Water heating + space cooling + space heating	A collector-evaporator and an air-source evaporator in parallel, a water-refrigerant plate heat exchanger connected with a radiant floor heating unit and two fan-coil units, an immersion condenser, a four-way valve	Five operating modes: space-heating-only mode, space-cooling-only mode, water-heating-only mode, space-heating and water-heating combination mode, space-cooling and water-heating combination mode Low or no solar radiation: the air-source evaporator in operation Summer: fan-coil units in operation, the collector-evaporator working as a condenser, the water-refrigerant plate heat exchanger working as an evaporator Winter: the radiant floor heating unit in use, the water-refrigerant plate heat exchanger working as a condenser	Experiments	Space-heating-only mode: COP varies 2.1-2.7 Space-cooling-only mode: COP = 2.9 Water-heating-only mode: COP varies 2.1–3.5 at a load temperature of 50 °C

Table 7
COP values for different operating mode of integrated SAHP for cooling, water heating and drying in a typical meteorological day.

	Full	NoWC	NoAC	NoRE	NoEC
Minimum	4.5	3.7	2.9	3.0	3.1
Maximum	6.5	4.4	7.6	4.2	3.7
Average	5.0	4.1	3.9	3.6	3.3

selection, the manufacture and assembly, and tests of the DX-SAHP system. There are still lack of specific international or national standards that guide designers and manufactures on how to develop a DX-SAHP system with good performance for different applications and various climates. As the consequence of the absence of standards, there are big differences in configuration (structure) parameters and operational performance of DX-SAHP systems existing in previous and current research. Without the standard guides, there is confusion about the development of commercial systems.

(3) *Exploring optimal control strategies.* It is well known that the performance of a DX-SAHP system is influenced greatly by the weather conditions and the user's load. For a multifunctional system, there are several operating modes in general, which increases the complexity and difficulty in operation control. Exploring optimal mode switching and control strategies is a critical subject to enable these novel systems to work in an automatic and efficient way under all conditions.

(4) *Gathering practical project experience.* The vast majority of experimental research is still limited in the laboratories. Actual operation conditions are usually far more complex and contingent than the laboratory conditions. Therefore, in order to overcome these limitations, it is essential to understand the long-term performance and the real behaviour of DX-SAHP systems through investigating practical projects. In the meantime, researchers can get extensive experience to solve problems in the real-world applications. This would make the DX-SAHP technology more attractive and competitive in the solar market in the future.

Acknowledgements

This work was done while Guo-Hua Shi was visiting at the University of Melbourne. The visit was supported by the program of China Scholarships Council (No.201606735054). The authors appreciate the support from the Natural Science Foundation of Hebei Province, China (E2016502027), the Fundamental Research Funds for the Central Universities in China (2017MS124), the Scientific Research Project of Education Department of Hebei Province, China (Z2015119) and the National Key R&D Program of China (No. 2017YFC0704200). The authors also gratefully acknowledge the support from the Department of Infrastructure Engineering, Melbourne School of Engineering, the University of Melbourne. The authors are particularly grateful to two anonymous reviewers and Mr. Yan Wang (China Architecture Design & Research Group) for their valuable comments and guidance on revising this paper.

References

[1] Sporn P, Ambrose E. The heat pump and solar energy. Proc of the world symposium on applied solar energy phoenix, US1955.
[2] Charters WWS, Taylor L. Some performance characteristics of a solar boosted heat pump. Refrig Sci Technol 1976;64:1–8.
[3] Franklin J, Saaski E, Yamagiwa A. A high efficiency, direct expansion solar panel. Proceedings of 1977 flat-plate solar collector conference. 1977. p. 187–95.
[4] Chaturvedi SK, Shen JY. Thermal performance of a direct expansion solar-assisted heat pump. Sol Energy 1984;33:155–62.
[5] Huang B, Chyng J. Integral-type solar-assisted heat pump water heater. Renew Energy 1999;16:731–4.
[6] Huang B, Lee C. Long-term performance of solar-assisted heat pump water heater. Renew Energy 2004;29:633–9.
[7] Scarpa F, Tagliafico L, Tagliafico G. Integrated solar-assisted heat pumps for water heating coupled to gas burners; control criteria for dynamic operation. Appl Therm Eng 2011;31:59–68.
[8] Huang B, Chyng J. Performance characteristics of integral type solar-assisted heat pump. Sol Energy 2001;71:403–14.
[9] Chyng J, Lee C, Huang B. Performance analysis of a solar-assisted heat pump water heater. Sol Energy 2003;74:33–44.
[10] Tagliafico LA, Scarpa F, Valsuani F. Direct expansion solar assisted heat pumps–A clean steady state approach for overall performance analysis. Appl Therm Eng 2014;66:216–26.
[11] Cervantes JG, Torres-Reyes E. Experiments on a solar-assisted heat pump and an exergy analysis of the system. Appl Therm Eng 2002;22:1289–97.
[12] Li Y, Wang R, Wu J, Xu Y. Experimental performance analysis and optimization of a direct expansion solar-assisted heat pump water heater. Energy 2007;32:1361–74.
[13] Mohanraj M, Jayaraj S, Muraleedharan C. Exergy analysis of direct expansion solar-assisted heat pumps using artificial neural networks. Int J Energy Res 2009;33:1005–20.
[14] Zhang D, Wu Q, Li J, Kong X. Effects of refrigerant charge and structural parameters on the performance of a direct-expansion solar-assisted heat pump system. Appl Therm Eng 2014;73:522–8.
[15] Sun X, Wu J, Dai Y, Wang R. Experimental study on roll-bond collector/evaporator with optimized-channel used in direct expansion solar assisted heat pump water heating system. Appl Therm Eng 2014;66:571–9.
[16] Huang B, Lee J, Chyng J. Heat-pipe enhanced solar-assisted heat pump water heater. Sol Energy 2005;78:375–81.
[17] Kuang Y, Sumathy K, Wang R. Study on a direct-expansion solar-assisted heat pump water heating system. Int J Energy Res 2003;27:531–48.
[18] Xu G, Zhang X, Deng S. A simulation study on the operating performance of a solar–air source heat pump water heater. Appl Therm Eng 2006;26:1257–65.
[19] Pei G. Study on photovoltaic-solar assisted heat pump system and multifunctional domestic heat pump system [PhD thesis] Hefei: University of Science and Technology of China; 2006. (In Chinese).
[20] Pei G, Ji J, He W, Sun W. Dynamic performance of PV/T solar-assisted heat pump system. Eng Sci 2006;8:49–56.
[21] Ji J, Liu K, Chow T-t, Pei G, He W, He H. Performance analysis of a photovoltaic heat pump. Appl Energy 2008;85:680–93.
[22] Ji J, He H, Chow T, Pei G, He W, Liu K. Distributed dynamic modeling and experimental study of PV evaporator in a PV/T solar-assisted heat pump. Int J Heat Mass Transf 2009;52:1365–73.
[23] Mastrullo R, Renno C. A thermoeconomic model of a photovoltaic heat pump. Appl Therm Eng 2010;30:1959–66.
[24] Fu H, Pei G, Ji J, Long H, Zhang T, Chow TT. Experimental study of a photovoltaic solar-assisted heat-pump/heat-pipe system. Appl Therm Eng 2012;40:343–50.
[25] Wu W, Liu Z, Chen L, Cheng Q, Zhao L. Performance analysis on a novel solar storage heat pump water heater integrated with collector/storage/evaporation. J Nanjing Normal Univ 2009;9:28–34. (In Chinese).
[26] Wei L, Wang L, Wu W. Experimental study on the operating characteristics of solar heat pump water heater integrated with collector, storage and evaporation. J Nanjing Normal Univ 2011;11:36–43. (In Chinese).
[27] Wu W, Wei L, Cheng Q, Wang L. Coefficient of performance of solar heat pump water heater with energy storage. J Jiangsu Univ 2011;32:667–71. (In Chinese).
[28] Wang L, Wu W, Zhang T, Li K. Experimental study on integrated solar heat pump water heater with paraffin as a medium. Build Sci 2014;30:35–40. (In Chinese).
[29] Wu W, Wang L, Su P, Zhang T, Zhang F. Performance comparison of solar heat pump system with different phase change materials. Trans Chin Soc Agric Eng 2014;30:184–91. (In Chinese).
[30] Wu W, Wang L, Zhang T. Comparative study on storage characteristics of the integrated solar heat pump water heater. Acta Energiae Solaris Sin 2015;36:2216–23. (In Chinese).
[31] Shi G-H. An LNG vaporisation method and system utilizing solar assisted heat pump. China Patent No.201610067782.X. (In Chinese).
[32] Kara O, Ulgen K, Hepbasli A. Exergetic assessment of direct-expansion solar-assisted heat pump systems: review and modeling. Renew Sustain Energy Rev 2008;12:1383–401.
[33] Hawlader M, Chou S, Ullah M. The performance of a solar assisted heat pump water heating system. Appl Therm Eng 2001;21:1049–65.
[34] Hawlader M, Chou S, Jahangeer K, Rahman S, KW EL. Solar-assisted heat-pump dryer and water heater. Appl Energy 2003;74:185–93.
[35] Hawlader M, Jahangeer K. Solar heat pump drying and water heating in the tropics. Sol Energy 2006;80:492–9.
[36] Kuang Y, Wang R. Performance of a multi-functional direct-expansion solar assisted heat pump system. Sol Energy 2006;80:795–803.
[37] Ye S. An integrated solar heat pump system for cooling, water heating and drying [PhD Thesis] Singapore: National University of Singapore; 2009.
[38] Chow TT, Pei G, Fong K, Lin Z, Chan A, He M. Modeling and application of direct-expansion solar-assisted heat pump for water heating in subtropical Hong Kong. Appl Energy 2010;87:643–9.
[39] Kong X, Zhang D, Li Y, Yang Q. Thermal performance analysis of a direct-expansion solar-assisted heat pump water heater. Energy 2011;36:6830–8.
[40] Fernández-Seara J, Piñeiro C, Dopazo JA, Fernandes F, Sousa PX. Experimental analysis of a direct expansion solar assisted heat pump with integral storage tank for domestic water heating under zero solar radiation conditions. Energy Convers Manag 2012;59:1–8.
[41] Facão J, Carvalho MJ. New test methodologies to analyse direct expansion solar assisted heat pumps for domestic hot water. Sol Energy 2014;100:66–75.
[42] Shi G-H. Research on the LPG vaporization system utilizing solar assisted heat pump

[PhD thesis] Beijing: North China Electric Power University; 2015. (In Chinese).
[43] Sun X, Dai Y, Novakovic V, Wu J, Wang R. Performance comparison of direct expansion solar-assisted heat pump and conventional air source heat pump for domestic hot water. Energ Procedia 2015;70:394–401.
[44] Deng W, Yu J. Simulation analysis on dynamic performance of a combined solar/air dual source heat pump water heater. Energy Convers Manag 2016;120:378–87.
[45] Zhou J, Zhao X, Ma X, Qiu Z, Ji J, Du Z, et al. Experimental investigation of a solar driven direct-expansion heat pump system employing the novel PV/micro-channels-evaporator modules. Appl Energy 2016;178:484–95.
[46] Kong X, Li Y, Lin L, Yang Y. Modeling evaluation of a direct-expansion solar-assisted heat pump water heater using R410A. Int J Refrig 2017;76:136–46.
[47] Morrison G. Simulation of packaged solar heat-pump water heaters. Sol Energy 1994;53:249–57.
[48] Anderson T, Morrison G. Effect of load pattern on solar-boosted heat pump water heater performance. Sol Energy 2007;81:1386–95.
[49] Yang J. Optimal design and economic analysis of the solar assisted heat pump water heater [master of science thesis] Nanchang: Nanchang University; 2007. (In Chinese).
[50] Scarpa F, Tagliafico LA. Exploitation of humid air latent heat by means of solar assisted heat pumps operating below the dew point. Appl Therm Eng 2016;100:820–8.
[51] Moreno-Rodríguez A, González-Gil A, Izquierdo M, Garcia-Hernando N. Theoretical model and experimental validation of a direct-expansion solar assisted heat pump for domestic hot water applications. Energy 2012;45:704–15.
[52] Moreno-Rodriguez A, Garcia-Hernando N, González-Gil A, Izquierdo M. Experimental validation of a theoretical model for a direct-expansion solar-assisted heat pump applied to heating. Energy 2013;60:242–53.
[53] Ooi FC. Analysis of a solar-assisted heat pump system [Master of Science thesis] Canada: University of Alberta; 1993.
[54] Aye L, Charters W, Chaichana C. Solar heat pump systems for domestic hot water. Sol Energy 2002;73:169–75.
[55] Chata FG, Chaturvedi S, Almogbel A. Analysis of a direct expansion solar assisted heat pump using different refrigerants. Energy Convers Manag 2005;46:2614–24.
[56] Son C-H, Oh H-K. Condensation pressure drop of R22, R134a and R410A in a single circular microtube. Heat Mass Transf 2012;48:1437–50.
[57] Faria RN, Nunes RO, Koury RNN, Machado L. Dynamic modeling study for a solar evaporator with expansion valve assembly of a transcritical CO 2 heat pump. Int J Refrig 2016;64:203–13.
[58] Chaturvedi S, Abdel-Salam T, Sreedharan S, Gorozabel F. Two-stage direct expansion solar-assisted heat pump for high temperature applications. Appl Therm Eng 2009;29:2093–9.
[59] Andresen B, Salamon P, Berry RS. Thermodynamics in finite time. Phys Today 1984;37:62–70.
[60] Sieniutycz S. Finite-time thermodynamics and thermoeconomics. first ed. London: Taylor & Francis; 1990.
[61] Torres-Reyes E, De Gortari JC. Optimal performance of an irreversible solar-assisted heat pump. Exergy An Int J 2001;1:107–11.
[62] Nuñez MP. Exergy analysis and optimization of a solar-assisted heat pump. Energy 1998;23:337–44.
[63] Scarpa F, Tagliafico LA, Bianco V. A novel steady-state approach for the analysis of gas-burner supplemented direct expansion solar assisted heat pumps. Sol Energy 2013;96:227–38.
[64] Chaturvedi SK, Mohieldin TO, Chen D. Second-law analysis of solar-assisted heat pumps. Energy 1991;16:941–9.
[65] Kuang Y, Wang R, Xu Y. Studies on the performance of a direct-expansion solar-assisted heat pump water heating system. J Eng Thermophys 2004;25:737–40.
[66] O'Dell M, Beckman W, Mitchell J. Solar heat pump systems with refrigerant-filled collectors. ASHRAE Transact 1983;89.
[67] Mitchell J. Design method and performance of heat pumps with refrigerant-illed solar collectors. J Sol Energ 1984;106:159.
[68] Chaturvedi S, Chiang Y, Roberts A. Analysis of two-phase flow solar collectors with application to heat pumps. J Sol Energ 1982;104:358–65.
[69] Zhao J, Liu L, Li L, Zhu Q, Tu F. Investigation into the use of R134a in a direct expansion solar assisted heat pump. J Tianjin Univ 2000;33:302–5. (In Chinese).
[70] Liu L, Que Y, Zhao J, Zhang H. Simulation analysis on a direct-expansion solar-assisted heat pump system. Fluid Mach 2008;36:67–71. (In Chinese).
[71] Liu L, Zhao J, Zhang H. Simulation study on the model of direct-expansion solar-assisted heat pump system. Acta Energiae Solaris Sin 2009;30:596–601. (In Chinese).
[72] Aziz W, Chaturvedi S, Kheireddine A. Thermodynamic analysis of two-component, two-phase flow in solar collectors with application to a direct-expansion solar-assisted heat pump. Energy 1999;24:247–59.
[73] Ito S, Miura N, Wang K. Performance of a heat pump using direct expansion solar collectors. Sol Energy 1999;65:189–96.
[74] Huang B, Lee C. Performance evaluation method of solar-assisted heat pump water heater. Appl Therm Eng 2007;27:568–75.
[75] Sun Z, Wang R, Li Y. Variable frequency operation control strategy for DX-SAHPWH based on simulation and experiments. Acta Energiae Solaris Sin 2008;29:1235–41. (In Chinese).
[76] He H, Ji J, Pei G, He W, Liu K. The numerical simulation base on a dynamic and distributed model for a photovoltaic solar assisted heat pump. Acta Energiae Solaris Sin 2008;29:1504–9. (In Chinese).
[77] Buker MS, Riffat SB. Solar assisted heat pump systems for low temperature water heating applications: a systematic review. Renew Sustain Energy Rev 2016;55. 399-13.
[78] Krakow K, Lin S. A solar source heat pump with refrigerant-cooled solar collectors for cold climates. Int J Refrig 1983;6:20–33.
[79] Chaturvedi S, Abazeri M. Transient simulation of a capacity-modulated, direct-expansion, solar-assisted heat pump. Sol Energy 1987;39:421–8.
[80] Chaturvedi S, Chen D, Kheireddine A. Thermal performance of a variable capacity direct expansion solar-assisted heat pump. Energy Convers Manag 1998;39:181–91.
[81] Chaturvedi S, Gagrani V, Abdel-Salam T. Solar-assisted heat pump–a sustainable system for low-temperature water heating applications. Energy Convers Manag 2014;77:550–7.
[82] Malali PD, Chaturvedi SK, Abdel-Salam TM. An approximate method for prediction of thermal performance of direct expansion-solar assisted heat pump (DX-SAHP) systems for water heating applications. Energy Convers Manag 2016;127:416–23.
[83] Hulin H, Xinshi G, Yuehong S. Theoretical thermal performance analysis of two solar assisted heat-pump systems. Int J Energy Res 1999;23:1–6.
[84] Kuang Y, Wang R. Experimental study on the direct-expansion solar-assisted heat-pump water heater. J Eng Thermophys 2005;26:379–81.
[85] Li Y, Wang R, Wu J, Xu Y. Experimental performance analysis on a direct-expansion solar-assisted heat pump water heater. Appl Therm Eng 2007;27:2858–68.
[86] Xu G, Zhang X, Zhao S. Performance of flat-plate PV/T integrated heat pump water heating system. CIE J 2012;63:136–41. (In Chinese).
[87] Li H, Yang H. Potential application of solar thermal systems for hot water production in Hong Kong. Appl Energy 2009;86:175–80.
[88] Huang W, Ji J, Xu N, Li G. Frosting characteristics and heating performance of a direct-expansion solar-assisted heat pump for space heating under frosting conditions. Appl Energy 2016;171:656–66.
[89] Dong X, Tian Q, Li Z. Energy and exergy analysis of solar integrated air source heat pump for radiant floor heating without water. Energy Build 2017;142:128–38.
[90] Hawlader M, Dey PK, Diab S, Chung CY. Solar assisted heat pump desalination system. Desalination 2004;168:49–54.
[91] Hawlader M, Amin ZM. Development of a solar assisted heat pump desalination system. Solar energy: research, technology and applications. Nova Science Publishers, Inc.; 2008. p. 427–55.
[92] Hawlader M, Amin ZM. Desalination of seawater using solar, ambient energy and waste heat from air conditioning. Desalin Water Treat 2012;42:235–40.
[93] Amin ZM, Maswood AI, Hawlader MNA, Al-Ammar EA, Orfi J, Al-Ansary HA. Desalination with a solar-assisted heat pump: an economic optimization. IEEE Systems Journal 2013;7:732–41.
[94] Amin ZM, Hawlader MNA. Analysis of solar desalination system using heat pump. Renew Energy 2015;74:116–23.
[95] Shi G-H, Jing Y-Y, Wang S-L, Zhang X-T. Development status of liquefied natural gas industry in China. Energy Policy 2010;38:7457–65.
[96] Morgan R. Solar assisted heat pump. Sol Energy 1982;28:129–35.
[97] Ito S, Miura N, Takano Y. Studies of heat pumps using direct expansion type solar collectors. J Sol Energ-T Asme. 2005;127:60–4.
[98] Ibrahim O, Fardoun F, Younes R, Louahlia-Gualous H. Review of water-heating systems: general selection approach based on energy and environmental aspects. Build Environ 2014;72:259–86.
[99] Asaee SR, Ugursal VI, Beausoleil-Morrison I. Techno-economic assessment of solar assisted heat pump system retrofit in the Canadian housing stock. Appl Energy 2017;190:439–52.